ALOIS MATHEW NGONYANI

MARINE BACTERIA AND THEIR ROLE IN POLYETHYLENE TEREPHTHALATE BIODETERIORATION AND BIOFRAGMENTATION

Faculdade de Ciências e Tecnologia

Erasmus Mundus Mestrado em Qualidade em Laboratórios Analíticos

2022

ALOIS MATHEW NGONYANI

MARINE BACTERIA AND THEIR ROLE IN POLYETHYLENE TEREPHTHALATE BIODETERIORATION AND BIOFRAGMENTATION

Erasmus Mundus Mestrado em Qualidade em Laboratórios Analíticos

Trabalho efetuado sob a orientação de:

Dr. Isabel Marín Beltrán

Prof. Maria Clara Costa

Faculdade de Ciências e Tecnologia

2022

MARINE BACTERIA AND THEIR ROLE IN POLYETHYLENE TEREPHTHALATE BIODETERIORATION AND BIOFRAGMENTATION

Declaration of Authorship

I declare I am the author of this work, which is original and unpublished. The sources consulted have been duly cited in the text and included in the list of references.

_____

(Alois Mathew Ngonyani)

ACKNOWLEDGEMENTS

I would like to express my sincere gratitude to my supervisor. Dr. Isabel Marín Beltrán, her dedication, and commitment of seeing her student successful had been of great contribution towards completion of this master thesis. Her intellectual advice, expert guidance, exhaustive scrutiny, moral and material support has been instrumental towards completion of this research. To be honest without her guidance, encouragement and tireless support this thesis would not have been possible. I am indebted for her forever. "Asante sana Isabel".

A debt of gratitude is also owed to my co-supervisor, Prof. Maria Clara Costa, her insightful and timely comments and suggestions, supervision, and constructive ideas has been vital towards completion of this thesis.

I would like to extend my sincere thanks to Prof. Bjørn Grung, Coordinator of the Erasmus Mundus Master in Quality in Analytical Laboratories (EMQAL) Program, for his guidance moral and material support during my studies.

I would like to extend my thanks to the European Union through Erasmus Mundus Scholarship for studentship that have allowed me to conduct this thesis and the Government of the United Republic of Tanzania, Government Chemist Laboratory Authority for allowing me to take part into this master's degree program.

I also acknowledge with many thanks a lot of support and cooperation I have received from all ECOREACH research group team and for a memorable time spent together in the lab, and in social settings.

Finally and more important, I would like to express my gratitude to my family, my beautiful wife Rebecca Allen Mwakajila, my son Derrick, my beautiful daughters Faina, Amariyah and Arianna for their love support and prayers. Without their tremendous understanding and encouragement in the past two years, it would be impossible for me to complete my study.

DEDICATION

I dedicate this thesis to my late parents Mr. and Mrs. Mathew Aaron Ngonyani, they are the reason for what I become today, May your soul continue resting in an eternal peace.

ABSTRACT

Microplastic (MP) pollution is a serious threat to the terrestrial and marine environment, posing a serious threat to all living beings. Therefore, there is an urgent need to find cheap, safe, and environmentally friendly solutions to alleviate the problem.This study aimed to assess the potential of a marine bacteria community and two of its isolates to biodegrade petroleum-based polyethylene terephthalate (PET) plastic bottles and bio-based polyethylene terephthalate (BPET) plastic bags. Ultraviolet (UV) treated microplastic films (~2 mm^2), were exposed to the consortium of bacteria and isolates for 90 and 45 days, respectively. Negative (MP without inoculum) and positive (bacterial inoculum, without any MP) controls were used in parallel. During the incubation period, samples were taken every two weeks or monthly to analyse bacterial growth, the pH, and changes in the polymer functional groups using Fourier Transform Infrared spectroscopy − Attenuated TotalReflectance (FTIR-ATR). The Chemical Oxygen Demand (COD) of microplastic was also measured at the beginning and at the end of the experiments. At the end of the incubation period, MP particles were subjected to scanning electron microscopy (SEM). Bacterial growth showed a statistically significant increase in the samples inoculated with marine bacteria as compared with the negative controls. The absorbance of peaks characteristic of the PET and BPET significantly decreased in the samples containing bacteria, and new peaks also appeared. Our results showed that marine bacteria have the potential to biodegrade petroleum-based and bio-based polyethylene terephthalate (BPET) MPs. These results further highlight the importance of rethinking bioplastics as an alternative to conventional plastics and how biological recycling can provide "green route" remedial solutions for PET microplastic polluted environment and consequently decreasing the environmental footprint of plastics.

Key words: microplastics, biodegradation, polyethylene terephthalate (PET), marine bacteria, FTIR-ATR, SEM.

Sumário

A poluição por microplásticos (MPs) é uma séria ameaça para o ambiente terrestre e marinho, representando um risco para todos os seres vivos. Portanto, há uma necessidade urgente de encontrar soluções baratas, seguras e ecológicas para aliviar o problema da poluição por MPs, e diminuir a pegada ambiental dos plásticos. Este estudo teve como objetivo avaliar o potencial de uma comunidade de bactérias marinhas e dois isolados para biodegradar garrafas de polietileno tereftalato (PET), e sacos plásticos feitos a partir de polietileno tereftalato de origem biológica (BPET). Filmes destes microplásticos (~2 mm^2) foram tratados com luz ultravioleta e expostos a um consórcio de bactérias e aos isolados por 90 e 45 dias, respectivamente. Controles negativos (MPs sem inóculo) e positivo (inóculo bacteriano, sem qualquer MP) foram usados em paralelo. Durante o período de incubação, foram coletadas amostras cada duas semanas ou mensalmente para analisar o crescimento bacteriano, o pH e as mudanças nos grupos funcionais dos polímeros, usando espectroscopia de infravermelho por transformada de Fourier − Reflectância Total Atenuada (FTIR-ATR). A Demanda Química de Oxigênio (DQO) dos microplásticos também foi medida no início e no fim das experiências No final do período de incubação, as partículas de MP foram ainda submetidas a microscopia eletrônica de varredura (MEV). O crescimento bacteriano apresentou um aumento estatisticamente significativo nas amostras inoculadas com bactérias marinhas em relação aos controles negativos. A absorbância dos picos característicos do PET e BPET diminuiu significativamente nas amostras contendo bactérias, e novos picos também apareceram. Os resultados mostraram que as bactérias marinhas apresentam um potencial para biodegradar PET MPs à base de petróleo e de orígem biológica. Estes resultados destacam a importância de repensar os bioplásticos como uma alternativa aos plásticos convencionais, e como a reciclagem biológica pode fornecer soluções corretivas de "rota verde" para ambientes poluídos por microplásticos (mais particularmente, de PET MPs) e, consequentemente, diminuir a pegada ambiental dos plásticos.

Key words: microplásticos, biodegradação, tereftalato de polietileno (PET), bacterias marinhas, FTIR-ATR, SEM.

Table of Contents

ACKNOWLEDGEMENTS ..... *i*

DEDICATION ..... *ii*

ABSTRACT ..... *iii*

Sumário ..... *iv*

List of Tables ..... *vii*

List of Figures ..... *viii*

List of Abreviations ..... *xi*

1.INTRODUCTION *1*

1.1. Objectives 8

1.2. Hypothesis 8

2.MATERIAL AND METHODS *8*

2.1. Preparation of inoculum 8

2.2. Selection of target microplastics 9

2.3. Degradation experiment with marine bacteria communities 11

2.4. Degradation experiment with marine bacteria Isolates 13

2.4.1 Isolation of the bacteria from the initial community 13

2.4.2. Biodegradation experiment with the isolates 14

2.5. Chemical and biological analysis 15

2.5.1. Optical density and pH analysis 15

2.5.2. FTIR-ATR spectroscopy analysis 16

2.5.3. Chemical Oxygen Demand (COD) 19

2.5.4. Scanning Electron Microscopy (SEM) 19

2.5.5. Bacterial community/Isolates identification 20

2.6. Statistical Analysis 22

3. RESULTS AND DISCUSSION *23*

3.1. FTIR-ATR spectra of PET/BPET MP (communities and isolates) 23
3.1.1. PET biodegradation with Bacteria Community #I18 and Isolates WC and YC 26
3.1.2 BPET biodegradation with Bacteria Community #I18 Isolates WC and YC 28
3.2. Optical density and pH analysis 39
3.2.1. Optical density 39
3.2.2. pH 41
3.4. DNA concentration and quality for bacterial community identification 49
3.4.1. DNA Concentration and Quality 49
3.4.2. Identification of bacteria 49
3.5. PET and BPET biodegradation/biofragmentation comparison 55
4. CONCLUSIONS *56*
5. REFERENCES *57*

List of Tables

Table 1. *Principal spectral absorption peak positions (cm^{-1}) of the functional groups characterizing PET/BPET polymers, according to the current literatures. 17*

Table 2. *Results of non-parametric Wilcoxon-test for the different variables measured in the samples containing PET MPs (K and samples containing the bacterial inoculum #I18) at the 95% level of statistical significance. *p<0.05; **p<0.01; ***p<0.001; n.s.: non-significant (p>0,05). 29*

Table 3. *Results of non-parametric Wilcoxon-test for the different variables measured in the PET samples (K and samples containing the bacterial inoculum WC) at the 95% level of statistical significance. *p<0.05; **p<0.01; ***p<0.001; n.s.: non-significant (p>0,05)..... 32*

Table 4. *Results of non-parametric Wilcoxon-test for the different variables measured in the PET samples (K and samples containing the bacterial inoculum YC) at the 95% level of statistical significance. *p<0.05; **p<0.01; ***p<0.001; n.s.: non-significant (p>0,05)..... 33*

Table 5. *Results of non-parametric Wilcoxon-test for the different variables measured in the samples containing BPET MPs (K and samples containing the bacterial inoculum #I18) at the 95% level of statistical significance. *p<0.05; **p<0.01; ***p<0.001; n.s.: non-significant (p>0,05). 34*

Table 6. *Results of non-parametric Wilcoxon-test for the different variables measured in the BPET samples (K and samples containing the bacterial inoculum WC) at the 95% level of statistical significance. *p<0.05; **p<0.01; ***p<0.001; n.s.: non-significant (p>0,05). 37*

Table 7. *Results of non-parametric Wilcoxon-test for the different variables measured in the BPET samples (K and samples containing the bacterial inoculum YC) at the 95% level of statistical significance. *p<0.05; **p<0.01; ***p<0.001; n.s.: non-significant (p>0,05). 38*

Table 8. *Bacterial Identification using 16S rRNA gene sequence analysis of the bacteria isolates 54*

List of Figures

***Figure 1**. Relative abundance (%) of bacterial taxa at genus level (class within parenthesis) from the original BPET MPs containing a marine bacterial inoculum (#I18). Alpha = Alphaproteobacteria; Cyano = Cyanobacteria; Delta = Deltaproteobacteria; Gamma = Gammaproteobacteria. 9*

***Figure 2.** PET MPs made from a water plastic bottle (A); BPET MPs made from a biobased plastic bag. 11*

***Figure 3.** Chemical structure of PET monomer. Adapted from Venkatachalam, et al.,(2012).... 11*

***Figure 4.** Scheme of the biodegradation experiment, consisting of 10 particles of each microplastic polymers (PET and or BPET) inoculated (10%) with the marine bacterial consortium I18 (PET/BPET-I18). Negative and positive controls were also used with either no inoculum (PET/BPET -K) or no MPs (I18) respectively. 12*

***Figure 5.** Marine Agar media plates with colonies displaying different morphologic characteristics. 14*

***Figure 6.** Scheme of the biodegradation experiment with the isolates, consisting of eight treatments. 20 particles of each MP type (PET and or BPET) were inoculated (10%) with the white or yellow colonies (PET/BPET+WC/YC). Negative and positive controls were also used, containing either no bacteria (PET/BPET-K), or only the inoculum (WC/YC) and no MPs, respectively. 15*

***Figure 7.** Nicolet iN10 MX -FTIR microscope used for the analysis of microplastic polymers.. 17*

***Figure 8.**Spectral profile of PET microplastics, as determined by FTIR-ATR. The plot shows the results of the spectrum of the negative control (PET-K, on the top) and the sample with the bacterial consortium (PET +I18, at the bottom) at the end of the experiment (T4), superimposed to the spectrum of PET microplastics at the beginning of the experiment (T0). 24*

***Figure 9.** Spectral profile of BPET microplastics, as determined by FTIR-ATR. The plot shows the results of the spectra spectrum of the negative control (BPET-K, on the top) and the sample with the bacterial consortium (BPET +I18, at the bottom) at the end of the experiment (T4), superimposed to the spectrum of BPET microplastics at the beginning of the experiment (T0).. 24*

***Figure 10.** Spectral profile of PET microplastics, as determined by ATR-FTIR. The plot shows the results of the spectra spectrum of the negative control (PET-K, on the top), a sample inoculated with the bacterial isolate WC (PET+WC, in the middle) and a sample inoculated*

with the bacterial isolate YC (PET+YC, bottom) at the end of the experiment (T3), superimposed to the spectrum of PET microplastics before the incubation (T0). *25*
Figure 11. *Spectral profile of BPET microplastics, as determined by ATR-FTIR. The plot shows the results of the spectra spectrum of the negative control (BPET-K, on the top), a sample inoculated with the bacterial isolate WC (BPET+WC, in the middle) and a sample inoculated with the bacterial isolate YC (BPET+YC, bottom) at the end of the experiment (T3), superimposed to the spectrum of PET microplastics before the incubation (T0).* *26*
Figure 12. *Results of the measurement of the optical density (at 660 nm) – as indicative of bacterial growth – throughout time in the different treatments. I18 and K stand for the positive (bacterial inoculum) and negative (microplastic particles, without bacteria) controls, respectively. Error bars represent the standard error from three replicates.* *40*
Figure 13. *Results of the measurement of the optical density (at 660 nm) – as indicative of bacterial growth – throughout time in the different treatments. WC and YC corresponds to the bacterial isolates inoculated to the microplastic samples. K stands for the negative control (microplastic particles, without bacteria). Error bars represent the standard error from three replicates.* *41*
Figure 14. *pH in the different treatments through incubation time. #I18 stands for the marine bacterial inoculate (positive control).* *42*
Figure 15. *pH in the different treatments through incubation time. WC and YC stands for the marine bacterial isolates (positive controls).* *43*
Figure 16. *Representation of COD measured at the end of the experiment (after 90 days of incubation) for 5 PET and BPET particles. BPET/PET+I18 stand for the samples inoculated with marine bacteria (inoculum #I18), while BPET/PET-K stand for the negative controls.*..... *45*
Figure 17. *Representation of COD measured at the end of the experiment (after 45 days of incubation) for 5 PET and BPET particles. BPET/PET+WC/YC stand for the samples inoculated with marine bacteria isolates WC and YC, while BPET/PET-K stand for the negative controls. 45*
Figure 18a-d. *Structural changes and adhesion of bacteria biofilms were observed in the surface of PET and BPET MPs particles exposed to bacterial consortia 18 (PET+I18 and BPET+I18), and to isolates (WC and YC), in comparison to the negative controls (PET-K and BPET-K). These changes include the presence of fractures, cavities and holes which were observed in the*

test samples (Figs. 18b and d; Figs. 19b and c; and Figs 20b and c), while the negative controls showed a smooth surface (Figs 18a and c;19a and 20a). 46
Figure 19. *SEM micrographs of PET MP films after 45 days of incubation with the marine bacterial isolates (labelled as YC and WC), compared to the controls (labelled as K). (a) PET surface of a control particle depicting a smooth surface with no bacterial colonization on the surface; b) PET particle exhibiting structural changes with the formation of fractures and aggregation of bacteria after it was incubated with WC; c) PET MPs exhibiting structure changes with the formation of holes, fractures scratches and aggregation of bacterial biofilms after it was incubated with YC.. ..... 47*
Figure 20. *SEM micrographs of BPET MP films after 45 days of incubation with the marine bacterial isolates (labelled as YC and WC), compared to the controls (labelled as K). (a) BPET surface of a control particle depicting a smooth surface; b) BPET MP/particle exhibiting structure changes and aggregation of bacterial biofilms after it was incubated with WC; c) BPET MPs exhibiting structure changes with the formation of holes, cracks and aggregation of bacterial biofilms after it was incubated with YC..... 48*
Figure 21*. Relative abundance quantification of bacteria Community #I18 using 16S rRNA sequencing, following a 90-days incubation with both PET and BPET MP (Class)..... 50*
Figure 22. *Relative abundance quantification of bacteria Community #I18 using 16S rRNA sequencing, following a 90-days incubation with both PET and BPET MP (genera). 51*
Figure 23. *Relative abundance quantification of bacteria Community #I18 using 16S rRNA sequencing, following a 90-days incubation with both PET and BPET MPs (Species)..... 51*
Figure 24. *Relative abundance (%) of bacterial taxa at genus level (class within parenthesis) developed in the positive controls (I18) and microplastic samples inoculated with I18 after 90 days of incubation. MP refers to the bacteria found attached to the microplastic particles, as compared to free bacteria found in the surrounding marine broth (B)..... 52*
Figure 25. *Phylogenetic tree based on based on Bayesian and Maximum likelihood analyses of 16S rRNA gene sequences. The two support values associated with each internal branch correspond to PPs and MLbs proportions, respectively. Branches in bold indicate a support of PP ≥ 0.95 and MLbs ≥ 70%. An asterisk on a bold branch indicates that this node has a support of PP = 1.0 and MLbs = 100. The tree was rooted using two species from the "Viridibacillus".*
..... 53

List of Abreviations

Bp-Base pair

BPET- Bio-Based Polyethylene terephthalate

CCMAR - Centre for Marine Sciences

CO_2 - Carbon dioxide

COD - Chemical Oxygen Demand

COVID-19 - Coronavirus disease

DNA- Deoxyribonucleic acid

EG - Ethylene glycol

EMQAL - Erasmus Mundus Master in Quality in Analytical Laboratories

FTIR-ATR - Fourier Transform Infrared spectroscopy − Attenuated Total Reflectance

GA - Glutaric acid

I18- Bacteria Community I18

MB- Marine Broth

MP- Microplastics

MSM - Mineral Salt Medium

NCBI- National Center for Biotechnology Information

NOAA - National Oceanic and Atmospheric Admnistration

OD - Optical Density

OECD - Organisation for Economic Co-operation and Development

PCR - Polymerase chain reaction

PET - Polyethylene terephthalate

POPs - Persistent Organic Pollutants

PPE - Personal Protective Equipment

rpm - revolution per minute

RNA - Ribonucleic acid

SDS - Sodium dodecyl sulfate

SEM - Scanning Electron Microscopy

TPA - Terephthalic Acid

UNESCO -United Nations Educational, Scientific and Cultural Organization

UV - Ultraviolet

WC - White colony

WEF - World Economic Forum

YC - Yellow colony

GA-Glutaric acid

1.INTRODUCTION

Plastic is a single word for a multi-faceted reality, encompassing a wide variety of polymers and additives with very different chemical and physical properties. These plastics are used for many different applications, including plastic objects, packaging, infrastructure, vehicles, paints, and textiles (Boucher, et al., 2020). Plastics are mainly made from raw materials that include petroleum (by-products of its refining process), natural gas, carbon, common salt and other natural products (House–Ambrosetti, 2014) and recently from plants like corns and sugarcane, however, plastics made from plants still represent only a small portion of overall production (The Globalist, 2015). Global plastics production was estimated at 367 million metric tons in 2020 (Plastics Europe, 2021; Tiseo, 2022). While this was a decrease from the previous year, global plastic production has almost doubled since the turn of the century and is set to continue growing due to rising populations, increased buying power, and further demands for plastic goods (Geyer, et al., 2017; Tiseo, 2022).

The rapid growth of plastics is due to their unique properties: high strength-to-weight ratio, high moldability, impermeability to liquids, resistance to physical and chemical degradation, and low cost, therefore, they can easily substitute for other materials (such as glass, metal, wood and natural fibres) in a wide range of applications (OECD, 2022; Tiseo, 2022). Some of these desirable qualities of plastics are also their key limitations. Plastics are highly resistant to physical and chemical degradation, which also means that they can persist as waste in the environment for decades or even centuries (OECD, 2022) leading to a serious environmental problems (Shamz, et al., 2011; Mohanan et al., 2020; Li, et al., 2022).

While concern about the environmental externalities of plastics had already emerged by the 1970s, when scientists started observing plastic leakage in the aquatic environment (OECD, 2022), an increase in global production of plastic and the low circularity of its economy has also contributed to the significant amount of plastic leaking into the environment each year (Boucher, et al., 2020; Marín-Beltrán, et al., 2022). According to Geyer et al. (2017), the quantity of global plastic waste produced between 1950 and 2015 is estimated to be 6.3 billion tons. Of this amount, only 9% has

been recycled, and 79% has accumulated in landfills or in the natural environment (Geyer et al., 2017). According to future estimations, 13.2 billion tons of plastic waste would still reach landfills and the environment (freshwater, oceans, air) by 2050 without the needed improvements of current plastic waste management (Shamz, et al., 2011).

Aside from macroplastics (i.e. plastics with a size of more than 5 mm) (Axelsson & van Sebille, 2017) debris exposed in the water bodies or land, a more threatening issue has been raised recently, is the widespread pollution of microplastics (MP). MP are primary or secondary small plastics with a diameter of less than 5 mm (Bretas Alvim, et al., 2020). MPs are considered primary when they enter the environment as microplastics (Rochman, et al., 2016) i.e. they are either industrially manufactured as microbeads of different sizes or as larger virgin plastics pellets (Andrady, 2017), while secondary MPs and the likely more significant source of MP, are formed when MP breaks down into micro-sized or nano-sized pieces (Rochman, et al., 2016) under various aging and or degradation/fragmentation processes when macroplastics are exposed to various environmental abiotic conditions, e.g., UV light, pH, salinity, and temperature in natural environments including marine, freshwater, land, atmosphere, and even North and South Poles (Zhang, et al., 2019; Fadare & Okoffo, 2020; Shamz, et al., 2011; Zhou, et al., 2021).

Oceans are now believed to be a major sink of MP (Woodall et al., 2014). Borrelle, et al., (2020), estimated that 19 to 23 million metric tons, or 11%, of plastic waste generated globally in 2016, entered aquatic ecosystems. The UNESCO (2022) reported that currently, there are about 50-75 trillion pieces of plastic and microplastics in the ocean. It is expected that these MP will be countinously generated in the future, due to several reasons: the high consumption of synthetic polymers (together with the inadequate management of subsequent residues), the insufficient disposal and recycling systems, and also the lack of public awareness regarding the issue (Bretas Alvim, et al., 2020).

Microplastics (MP) are deemed the most harmful to humans and living organisms, particularly when present under marine conditions (Dimassi, et al., 2022). Given their extremely small size, MPs can easily be ingested by various marine species organisms (Yuan, et al., 2022). Ingestion of MPs by marine oranisms lead to blockage of digestive tract followed by satiation, starvation and

general debilitation often leading to death, reduction in quality of life and reproductive capacity, drowning and limited predator avoidance and impairment of feeding capacity; and the possibility that plastic resin pellets may adsorb and concentrate potentially damaging toxic compounds from sea water (Gregory, 2009) and further may or be translocated into the circulatory system (Browne, et al., 2008). Ingestion of MP by amphipods, lugworms, sea cucumbers, and mussels that have been exposed to microplastics has been previously reported (Thompson, et al., 2004; Browne, et al., 2008; Gouin, etal., 2011; Cole, et al., 2013).

In addition to that, ingestion of MP provides a potential pathway for the transfer of pollutants, monomers, and plastic additives to organisms with uncertain consequences for their health and then these MPs could be accumulated in higher trophic level species, including humans (Gourmelon, 2015; Gong, et al., 2018; Hatzonikolakis, et al., 2022; Yuan,et al., 2022). Research estimates that the humans intake of MP through the ingestion of food and water contaminated with these particles is up to 142,000 MPs/year (Van Cauwenberghe & Janssen, 2014; Cox, et al., 2019; Torena, et al., 2021). Moreover, any potential accumulation of these fine pieces is a major concern since they are characterized as persistent organic pollutants (POPs) that will further burden humans, living organisms (especially marine), and the environment, considering the potential carcinogenicity of the chemicals they bear (Hahladakis, et al., 2018; Chen, et al., 2019; Dimassi, et al., 2022).

MP also affect phytoplankton photosynthesis (WEF, 2022). Phytoplankton is the primary producer of ocean, and it can utilize CO_2 adsorbed from the atmosphere or ocean to produce organic matters and O_2 by photosynthesis mitigating level rise of atmospheric CO_2 and global warming (Shen, et al., 2019). Marine primary production approximately accounts for 50 - 80% of the total oxygen production of the earth (NOAA, 2021). A large amount of MP floating on oceans can affect the light transmission, thereby influencing the efficiency of phytoplankton photosynthesis. Once the ability of oceans for CO_2 sequestration is disturbed, the global carbon cycle pattern will dramatically change, thus threatening the basic conditions for human survival (Shen, et al., 2019). In addition to that, zooplankton consumption of MP also reduces the grazing on primary producers and this could further accelerate the loss of ocean oxygen (Kvale, et al., 2021). Therefore, the surging contamination of the marine environment by MP is of concern not only because of the

ecological impacts but also because they may compromise food security, food safety and consequently human health (Gong, et al., 2018 ;Yuan, et al., 2022).

The coronavirus that is the cause of an infectious disease known as COVID-19, first discovered in Wuhan in the People's Republic of China in December 2019, spread to other countries and continents in less than a few months and triggered a global health pandemic. Governments responded to the emerging crisis with a range of measures to contain the spread, especially limiting the movement of people and goods and shutting down economic activity (OECD, 2022).

Plastic also have played a significant role to safety of people from communicable diseases (Kumar, et al., 2021; Fadare & Okoffo; 2020; Li, et al., 2021). The COVID-19 pandemic has also highlighted the importance of plastics in our daily lives. A range of personal protective equipment (PPE) such as surgical face masks, single-use medical tools and packaging made from plastics have played crucial roles in protecting people during the COVID-19 pandemic with a focus on healthcare workers and other frontline personnel globally, millions of PPE were being produced and consumed daily for protection against the deadly COVID-19 virus (Fadare & Okoffo, 2020; Olatayo, et al., 2021; Benson, et al., 2021). Single-use plastic items such as face masks and medical tools can reduce the potential spread of diseases and viruses effectively, as long as they are disposed of in a sanitary manner (OECD, 2022).

Disruptions in supply chains due to lockdowns and border restrictions reduced plastics production overall. Plastics Europe (2021) and Tiseo (2022) estimated that production decreased by roughly 0.3 percent in 2020 as compared to 2019". There are also big regional differences in the economic effects of the pandemic, and lockdown measures varied widely across countries. Thus, the changes in plastics production varied across countries (OECD, 2022). The COVID-19 pandemic had mixed effects on the demand for packaging in the year 2020. On the one hand, the shift towards take - away, food delivery and e-commerce increased demand for plastic packaging. The demand for hygiene products, including disinfectant gel which mostly comes in plastic packaging also increased. On the other hand, the closure of shops and workplaces and other limitations to economic activity translated into reduced demand for packaging (OECD, 2022).

As lockdowns took effect to slow the spread of the pandemic, the global demand for petroleum collapsed. As a result, oil prices plummeted, making the manufacture of virgin plastics from fossil fuels less expensive than recycling. This cost incentive, along with lifestyle changes that increased plastic use, has complicated the challenge of overcoming plastic pollution (Adyel, 2020). The combat against the pandemic has resulted in, and continues to yield, vast amounts of waste. Particularly medical waste, but also household waste, the composition of which is greatly affected by disposable plastic-based PPE and single-use packaging plastics, stemming from the noted surge in online shopping (Pinto da Costa, 2021; Parashar & Hait, 2011), intensifying pressure on waste managment (Peng, et al., 2021).

The natural environment, which at the beginning of the pandemic benefited from reducing litter and improved water quality from decreased tourism, are now becoming tainted with COVID 19 - related waste (Patrício Silva, et al., 2021; Olatayo, et al., 2021). Peng, et al. (2021) reported that more than eight million tons of pandemic-associated plastic waste have been generated globally, with more than 25,000 tons entering the global ocean. In addition to that, Benson et al. (2021) estimated that approximately 3.4 billion single-use facemasks or face shields are discarded daily since the start of the COVID-19 pandemic. It is further estimated that, if the global population adheres to a standard of one disposable face mask per day after lockdowns end, the pandemic could result in a monthly global consumption and waste of 129 billion face masks and 65 billion gloves (Adyel, 2020).

Among all plastic types, polyethylene terephthalate (PET), produced by the polymerization of ethylene glycol (EG) and terephthalic acid (TPA), is widely used in textiles or packaging due to its excellent properties in terms of durability, lightness, plasticity, and low price (Li, et al., 2022; Son, et al., 2021). While the annual production of PET is predicted to exceed 70 million tons (Euginio, et al., 2021) in 2020, up to 90 % of post-consumed PET enters terrestrial and oceanic ecosystems as wastes, posing a serious threat to the environment and human health (Nimchua, et al., 2007; Dai, et al., 2021). Even though recycling systems are in place (e.g., for the PET bottles market), over half of the PET that is produced globally escapes collection, and instead ends up in landfills or is released into the environment and is projected to persist for hundreds of years (Carr, et al., 2020; Liu, et al., 2021). Therefore, there is an urgent demand for the development of cost-

effective green approaches to control PET pollution to protect the global ecosystem (Dai, et al., 2021).

Currently, the recycling of PET has been considered the best approach to resolve the PET waste problem. Several strategies have been developed to recover used PET including chemical, physical, and biological treatments. Among them, physical recycling is a relatively simple and inexpensive method by direct converting PET into new end products through physical treatments like cutting, heating, or extrusion (Carr, et al., 2020). In an industrial context, PET can be depolymerized to its constituents via chemistries able to cleave ester bonds. However, to date, few chemical recycling solutions have been deployed, given the high processing costs relative to the purchase of inexpensive virgin PET. This, in turn, results in reclaimed PET primarily being mechanically recycled, ultimately resulting in a loss of material properties and hence intrinsic value. Given the recalcitrance of PET, the fraction of this plastic stream that is landfilled or makes its way to the environment is projected to persist for hundreds of years (Austin, et al., 2018).

In response to the issue of surging PET pollution and to decrease the environmental footprint of PET, more particularly MPs, there is an urgent need to find cheap, safe, and environmentally friendly solutions to alleviate the problem of plastic pollution and decrease the environmental footprint of plastic. In recent years, bioremediation has attracted lots of attention since it can provide a “green route” for recycling PET with several advantages, such as easy operation, environmentally friendly, energy savings, and minimizing waste. In this terms, a few microorganisms with the ability to grow in PET wastes have been recently discovered (Chen, et al., 2020; Janczk, et al., 2020; Sanniyasi et al., 2021).

These microbes can degrade PET plastics with ester bonds via enzymatic hydrolysis through colonization onto the surfaces of materials. The degree of biodegradability of plastics depends on their chemical and physical properties (Joo, et al., 2018; Oliveira, et al., 2020). Several bacterial hydrolases that can catalyze PET by hydrolysis have been discovered in the past few years including cutinase (Sheng, et al., 2008), lipase (Nechwatal, et al., 2006; Sulaiman, et al., 2011), esterase (Austin, et al., 2018; Ribitsch, et al., 2011; Sharon & Sharon, 2012) and carboxylesterase

(Billig, el al., 2010), have been identified as promising environmental biocatalysts to alternate chemical and physical recycling of PET (Carr, et al., 2020; Jia, et al., 2021; Dai, et al., 2021).

Apart from the potential use of microorganisms to reduce the plastic waste problem, biobased and biodegradable plastics are currently being developed to reduce the use of conventional, petroleum-based plastics and are expected to offer solid alternative to petrochemical plastics in the near fucture (Steven, et al., 2020; Moshood, et al., 2022). Among these, are biobased plastics, materials (partially) developed from renewable feedstocks (European Bioplastics, 2018). Compared to their conventional counterparts, biobased plastics have two major advantages. Firstly, they save fossil resources by using plant-based sources such as corn, sugarcane and cellulose which regenerates annually and, secondly, they provide the unique potential of carbon neutrality (European Bioplastic, 2018). According to Raushan, et al. (2022) biobased plastics have the potential to reduce 30 - 70% of carbon dioxide emission, it represents approximately 42% reduction of carbon footprints, and their production requires 65% less energy than conventional petroleum plastic.

The adoption of biobased plastic has increased tremendously across various applications, owing to the advanced technical properties and functionalities (Raushan, et al., 2022). The demand for biobased plastics has gained incredible traction in various plastic applications due to the favorable legislation implemented by numerous governments around the globe (Raushan, et al., 2022). However, to date, biobased plastic still represent less than one percent of the more than 367 million tonnes of plastic produced annually (Plastics Europe, 2021). Moreover, compared to conventional plastics, there is still no solid evidence that these plastics would break down in the natural environment (Shamz, et al., 2011; Jeon et al., 2021). Furthermore, both the production scale and usage of biobased plastics are still very limited due to their low durability and lack of supporting systems (Dang, et al., 2018). The high final cost of bioplastic products is also another factor that hinders the growth of the bioplastic market, bioplastics are more than twice expensive when compared to conventional, petroleum-based, plastics (Raushan, et al, 2022). To date, there are quite a few studies on the biodegradability of conventional PET MP (Auta, et al., 2017; Mecozzi & Nisini, 2019; Farzi, et al., 2019), which account for 10.2% of the total global conventional plastic production (Geyer, etal., 2017). However, only few studies have focused on the biodegradation of bio-based PET MPs (Mecozzi & Nisini, 2019; Fernández de Villalobos et al. 2022).

1.1. Objectives

This study, as part of the European master's degree of Quality in Analytical Laboratories (EMQAL), is aimed to find marine bacteria with the potential to biodegrade petroleum-based (PET) and bio-based polyethylene terephthalate (BPET). For this, PET and BPET microplastic particles were subjected to bacterial communities and isolates, and physico-chemical changes in the properties of the two polymers were evaluated through time. These included changes in the physical and chemical properties of the particles by specific techniques such as Scanning Electron Microscopy (SEM) and Fourier Transform Infrared Spectroscopy (FTIR).

1.2. Hypothesis

Based on results from previous work with a bacterial community developed on BPET MP films (Fernández de Villalobos et al., 2022), we expect a low biodegradation rate of BPET and PET. Still, a higher degradation of BPET, as compared to conventional PET is expected, since biobased or oxo-degradable PET contain additives that accelerate the oxidation process (prodegradants) (Ammala, et al., 2011; Kubowicz & Booth, 2017).

2.MATERIAL AND METHODS

2.1. Preparation of inoculum

A community of marine bacteria which had grown onto biobased polyethylene terephthalate (hereafter referred as BPET) microplastic films in a previous experiment (for details, see Fernández de Villalobos et al., 2022), was used in this experiment as the initial community to assess its potential to biodegrade BPET and conventional, petroleum-based, polyethylene terephthalate (hereafter referred as PET). This community of bacteria had its origin in the tunicate *Didemnum* sp., a sample of which was collected in July 2020 from the Catedral cave (37º00'63.86" N, 8º92'74.24" W), close to the city of Sagres, in southern Portugal. The community of bacteria had been recovered from three different replicates containing BPET microplastic (MP) films after 45 days of incubation in the dark, at room temperature (25±2°C), under orbital agitation (150 rpm). Bacteria were recovered from the BPET MPs using a commercial DNA extraction kit (DNeasy®

PowerSoil Pro Kit, QIAGEN, Germany), and had been stored at -20 °C for 6 months. Then, the samples were thawed and the bacterial inoculum was prepared by adding one aliquot of these samples to a flask containing an artificial, sterile, marine broth (PanReac) (1:10 dilution). The sample was then incubated in the dark, at ±25°C, under orbital agitation (150 rpm). After 48h of incubation, bacteria samples were centrifuged (4000 rpm; 10 minutes); the supernatant was discarded, and the pellet was washed and resuspended in new marine broth. The washing procedure was then repeated three times, and the final pellet was resuspended in the sterile marine broth and used as inoculum in the experiments (hereafter referred as inoculum #18). Common bacteria found in the inoculum are shown in Fig. 1.

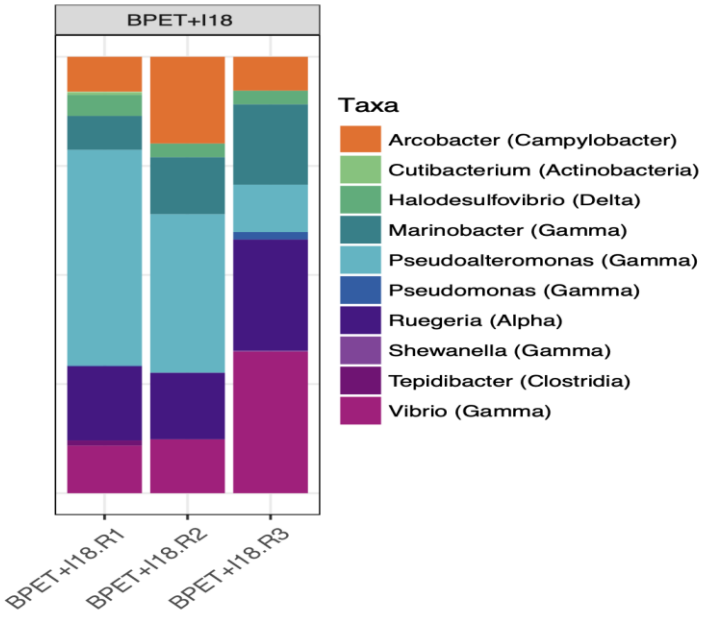

Figure 1. Relative abundance (%) of bacterial taxa at genus level (class within parenthesis) from the original BPET MPs containing a marine bacterial inoculum (#I18). Alpha = *Alphaproteobacteria*; Cyano = *Cyanobacteria;* Delta = *Deltaproteobacteria*; Gamma = *Gammaproteobacteria*.

2.2. Selection of target microplastics

PET MP films were obtained from a conventional plastic water bottle from a supermarket, and BPET MPs from a commercially available plastic bag from a local shop labeled as "biodegradable". According to the Plastics Europe classification (European Bioplastics, 2018),

there is currently no PET classified as “biodegradable”. We therefore understand that this bag was made instead of “biobased” PET, which presents the same chemical structure than conventional PET. PET and BPET products were then manually cut, with scissors and a cutter, into MP films of an approximate area of 2 mm^2 (Fig.2), under sterile conditions. Both MP particles were sterilized afterwards by means of ultraviolet radiation (253, 7 nm) for 30 minutes before their use in the experiments, since this sterilization method was proven the best to avoid the growth of microorganisms (Fernández de Villalobos et al., 2022).

The chemical structure of PET is composed of repeating ($C_{10}H_8O_4$) units as shown in Fig 3. Each unit has a physical length of about 1.09 nm and a molecular weight of ~200 Da (Venkatachalam, et al., 2012). As shown in Fig. 3, the PET monomer consists of an aromatic ring coupled with a short aliphatic chain (Reese, 2003; Fotopoulou & Karapanagioti, 2017). PET is also characterized by a high ratio of aromatic terephthalate units and is also semicrystalline, consisting of both crystalline and amorphous domains (Taniguchi, et al., 2019). Knowing the molecular structure of the target polymers is essential for the study, since the degradation process of polymers depends, among other environmental factors, on its molecular weight, the reactive functional groups in the backbone, chain mobility/flexibility, degree of crystallinity, and surface hydrophobicity (Zheng, et al., 2005; Fotopoulou & Karapanagioti, 2017; Tiwari, et al., 2018;Taniguchi, et al., 2019; Ahmaditabatabaei, et al., 2021).

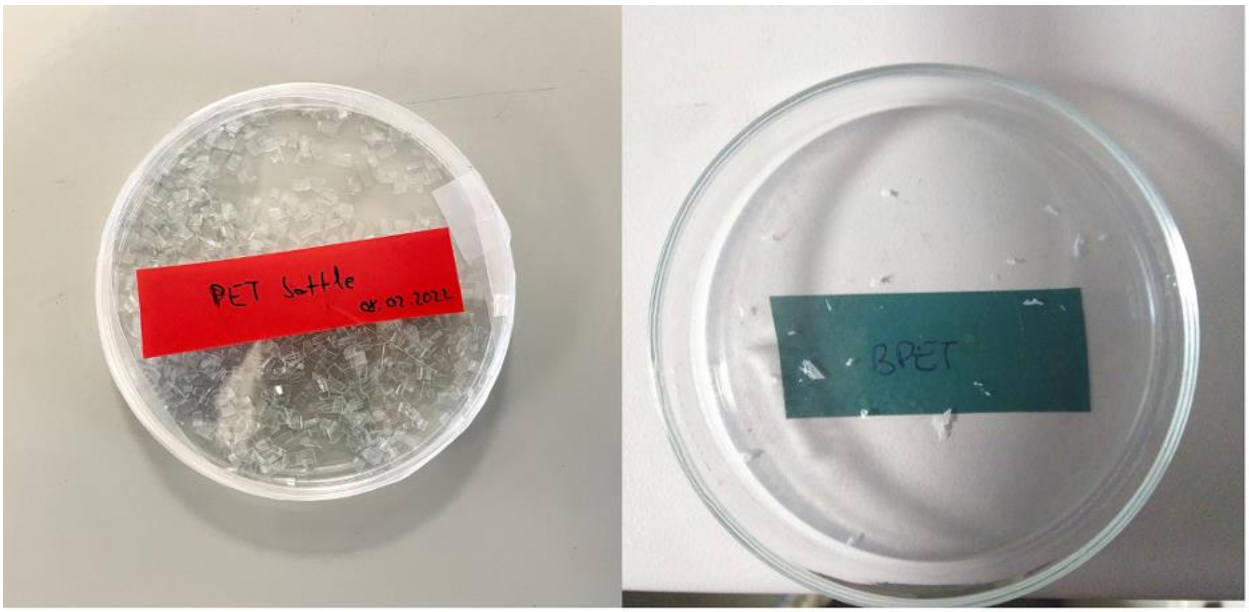

Figure 2. Polyethylene terephthalate (PET) microplastics made from a water plastic bottle (A); Polyethylene terephthalate microplastics made from a biobased plastic bag (labeled as BPET hereafter).

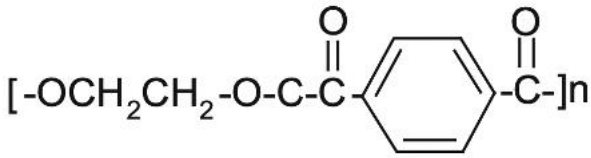

Figure 3. Chemical structure of polyethylene terephthalate monomer. Adapted from Venkatachalam, et al. (2012)

2.3. Degradation experiment with marine bacteria communities

Communities of marine bacteria which were found attached to BPET MP films in a previous experiment were used for this study (see section 2.1 and Fig. 1), and are here referred as "inoculum 18" (I18). The experiment was performed in liquid marine broth (MB), autoclaved before use, added to autoclaved glass flasks of 30 mL. The experiment consisted of 5 treatments, including

the experimental treatments and two types of controls. Sample treatments consisted of 10, UV-treated, PET and BPET MP particles inoculated with 10% v/v of initial bacterial community, contained in 10 mL of MB (final concentration 1000 MP L^{-1}). Two negative controls were used, one for PET and another for BPET samples. Each of these controls included MPs of each type, without any bacterial inoculum, at the same concentration of 1000 MP L^{-1}. There was also a positive control, containing 9 mL of marine broth with 10% v/v of the inoculum, without any MPs. Each treatment was performed in triplicate.

The samples were incubated in the dark, at 25±1°C, under orbital agitation (160 rpm). Sampling was performed at four different time intervals i.e., 14, 28, 56, and 90 days after the inoculation. An extra replicate (with a total of 4) was used at the end of the experiment (after 90 days of incubation), the whole experiment consisting of 65 samples. At each sampling time, samples were taken to analyze bacterial growth, the pH, and changes in the polymer functional groups using Attenuated Total Reflectance-Fourier Infrared spectroscopy (ATR-FTIR). The Chemical Oxygen Demand (COD) of the microplastic particles was measured at the beginning (after 14 days of incubation) and at the end of the experiment. After 90 days of incubation, particles of each experiment were also subjected to scanning electron microscopy (SEM). In addition, Deoxyribonucleic acid (DNA) was extracted from the MPs and the broth at the end of the experiment, to look for possible changes in the initial bacterial community attached to the particles.

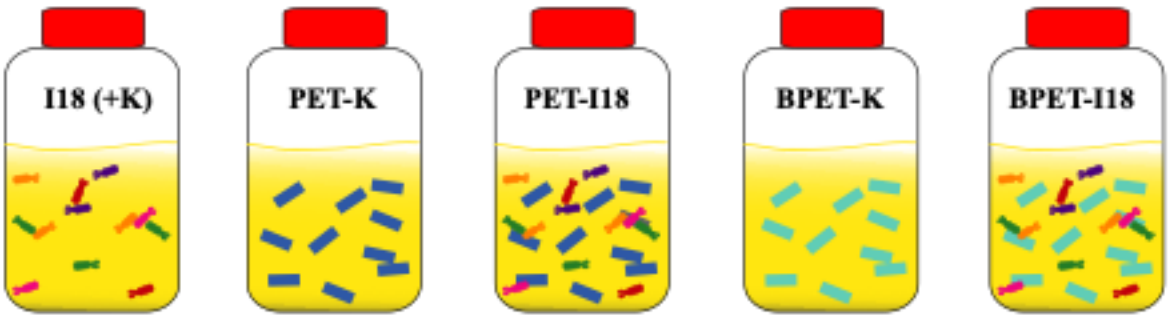

Figure 4. Scheme of the biodegradation experiment, consisting of 10 particles of each microplastic polymers (PET and or BPET) inoculated (10%) with the marine bacterial consortium I18 (PET/BPET-I18). Negative and positive controls were also used with either no inoculum (PET/BPET -K) or no MPs (I18) respectively.

2.4. Degradation experiment with marine bacteria Isolates

2.4.1 Isolation of the bacteria from the initial community

Our initial bacterial community, recovered from BPET microplastics (see sections 2.1 and 2.3), was further used for the growth of bacterial isolates, in order to assess the potential of the different members of this community on the biodegradation of PET and BPET. For this, I18 was added in Mineral Salt Media (MSM) (20 particles of the selected MPs) and Marine Broth (MB), (10 particles of the selected MPs) at concentration 10% v/v, as a 1st enrichment. After seven days, the bacteria were detached from the plastic particles by stirring for 3 minutes and two serial dilutions were prepared from the first enrichment (10^{-1} and 10^{-2}). 100 µl from the original culture and the two dilutions were then added to plates containing marine agar for the isolation of the bacteria strains. The remaining solution was kept for a second enrichment, adding 10% of the volume to new MSM and MB. The bacteria were isolated using colony morphotypes, a common method in microbial ecology to isolate different species for physiological and genetic purposes (Martinez, et al., 1996; Lebaron, et al., 1998). After 48 hours, 2 different morphotypes were identified in all the plates, and cultured in triplicates for isolation in new plates containing marine agar. After 48 hours, the two morphotypes were properly isolated, one of them showing bigger, white colonies, with irregular borders (hereafter refered to as "WC"), and another yellow, smaller and rounded colonies (hereafter refered to as "YC") (Figure 5). Three colonies from each isolate were picked up and resuspended in 20 mL of MB or MSM containing 40 PET or BPET MPs. The plates were then incubated at 25°C±1 and optical densities were recorded after 1, 2 and 5 days of incubation (Lebaron, et al., 1998; Saimmai, et al., 2012; Auta, etal., 2017). After that, they were used for DNA extraction (Lebaron et al. 1998; Palma, et al., 2021) and for the biodegradation experiment. Since recorded optical densities were quite low, (0.01%) v/v of Glycerol was added to the samples to facilitate the growth of the isolates and to adjust the optical density (OD) close to 1 at 660 nm. 5mL of cell culture of each isolate with optical densities $OD_{660} > 1$ and or close to 1 was used for DNA extraction and for biodegradtion experiments, as in previous studies (e.g. Auta, et al., 2017).

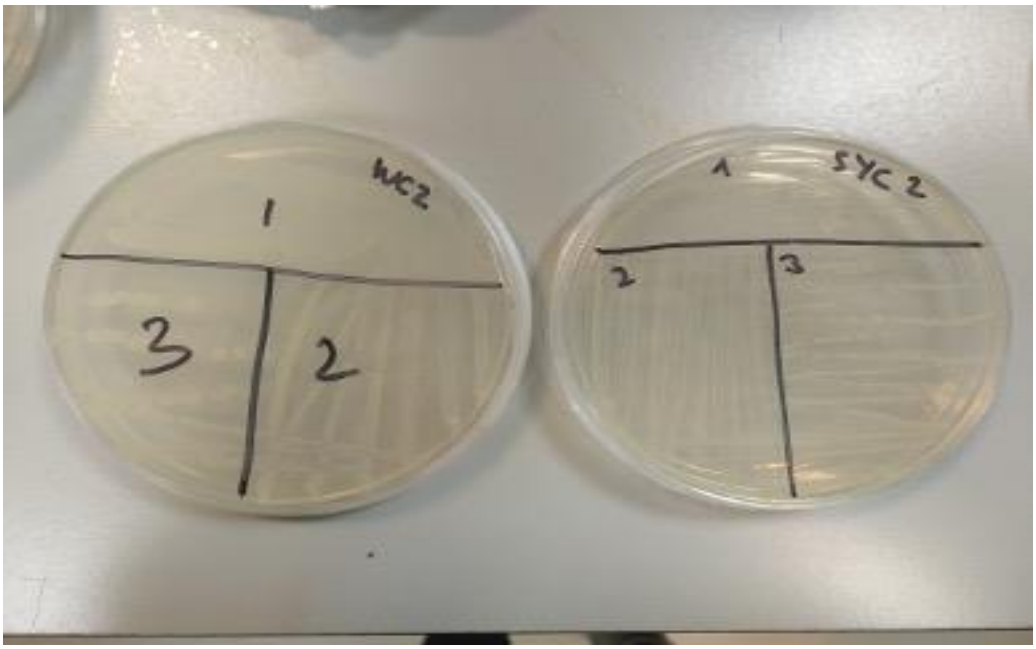

Figure 5. Marine Agar media plates with colonies displaying different morphologic characteristics.

2.4.2. Biodegradation experiment with the isolates

The experimental setup with the isolates was similar to that with the communities, except that this experiment was performed for 45 days, in MSM, adding 20 particles of each MP polymers (PET and or BPET) to guarantee that bacterial growth is not limited. The experiment consisted of 8 treatments, including 2 negative controls (one for each type of polymer) and 2 positive controls (one for each isolate). Experimental treatments consisted of PET particles inoculated with each type of isolate, and BPET particles enriched with each type of isolates. All treatments were performed in triplicate, having a total of 72 samples (Figure. 6). Sampling was performed at 3 times (i.e., at 14, 28 and 45 days). At each sampling time, samples were taken to analyze bacterial growth, the pH, and changes in the polymer functional groups using Attenuated Total Reflectance-Fourier Infrared spectroscopy (FTIR-ATR). The Chemical Oxygen Demand (COD) of the microplastic particles was measured at the beginning (after 14 days of incubation) and at the end of the experiment. After 45 days of incubation, particles of each experiment were also subjected to scanning electron microscopy (SEM). In addition, DNA was extracted from the MPs and the broth at the end of the experiment, to look for possible changes in the initial bacterial community attached to the particles.

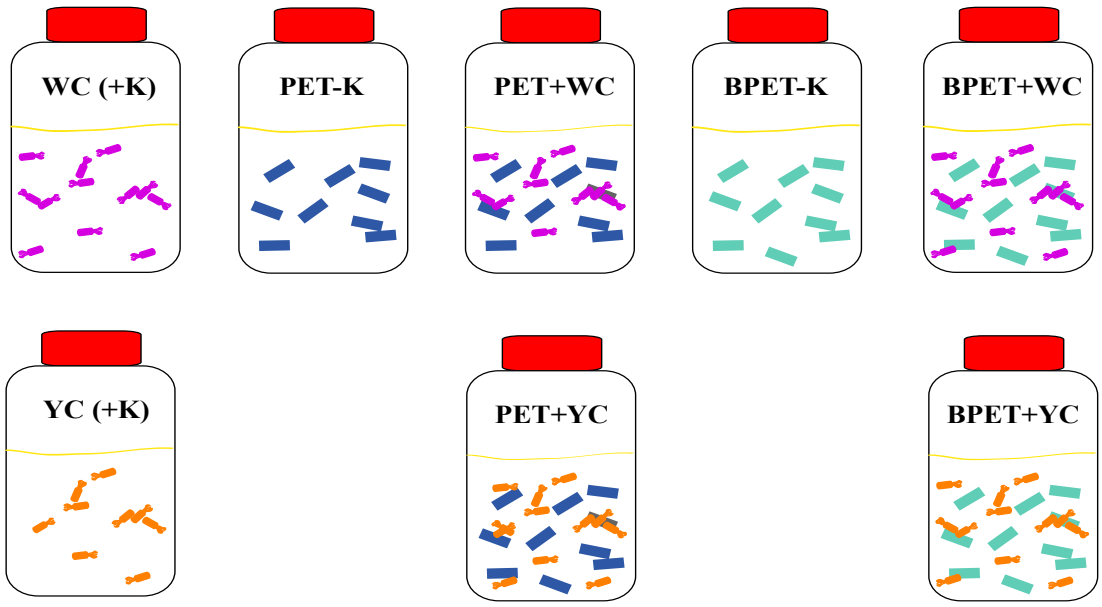

Figure 6. Scheme of the biodegradation experiment with the isolates, consisting of eight treatments. 20 particles of each MP type (PET and or BPET) were inoculated (10%) with the white or yellow colonies (PET/BPET+WC/YC). Negative and positive controls were also used, containing either no bacteria (PET/BPET-K), or only the inoculum (WC/YC) and no MPs, respectively.

2.5. Chemical and biological analysis

2.5.1. Optical density and pH analysis

In both, experiments with communities and isolates, three replicates were taken at each sampling time to analyse bacterial growth, by means of optical density (OD), and pH. Bacterial growth was assessed by measuring the absorbance of each replicate at 660 nm, using a Hach-Lange™ DR 2800 spectrophotometer (Sköndal, Sweden). The marine broth (communities) or MSM (isolates) were used as zero value. pH is a selective environmental factor affecting microbial diversity and activity, controlling enzyme activity, transport process, and nutrient solubility (Dhote , eat al., 2010). Therefore, effective polymer biodegradation is dependent on pH (Maurya, et al., 2020 ; Sarkhel,

et al., 2020; Hirota, et al., 2020) and changes in pH may be indicative of polymer biodegradation (Auta, et al., 2022). pH was measured using a pH-meter (CRISON, GLP21, Spain).

2.5.2. FTIR-ATR spectroscopy analysis

Fourier transform infrared spectroscopy (FT-IR) offers a simple, efficient, and non-destructive method for identifying and distinguishing most plastic polymers, based on well-known infrared absorption bands representing distinct chemical functionalities present in the material (Jung, et al., 2018). FTIR spectroscopy, coupled with Attenuated Total Reflection (FTIR-ATR) has proved to be a powerful tool to investigate the surface structural changes of PET microplastic polymers (Auta, et al., 2017; Jung, et al., 2018; Denaro, et al., 2020)

FTIR measurements were performed before the MP films were incubated, and then at each sampling time. Analysis were performed by measuring the spectra of 2 or 3 MP particles from each replicate and treatment (both types of MPs inoculated with marine bacteria and negative controls), using a Thermo Scientific Nicolet iN10 MX-FTIR microscope (Thermo Fisher Scientific; USA), operating in ATR mode (Fig. 4). The ATR crystal was made of germanium, this device allowing for a higher sensitivity of the spectra. A Mercury Cadmium Telluride (MCT) detector cooled with liquid nitrogen was used, which operates over the middle infrared region from 4000 to 675 cm^{-1}. Spectra were collected at the interval of 5 s, in absorbance mode, recording 16 scans at 16 cm^{-1} spectral resolution. Prior to FTIR-ATR analysis, MP particles were recovered from the Marine Broth through filtration using cellulose filters (25 µM). To facilitate accurate PET/BPET FTIR-ATR analysis of the bacterial film colonizing the PET /BPET surface was removed by washing the particles with a 2% (v/v) aqueous sodium dodecyl sulfate (SDS) solution (Harshvardhan & Jha, 2013) for 4 hours at room temperature; further with distilled water; then ethanol followed with drying in a hot air oven at 60 °C for 10 minutes. Table 1. shows the most characteristic absorbance peaks of PET/BPET according to the literature.

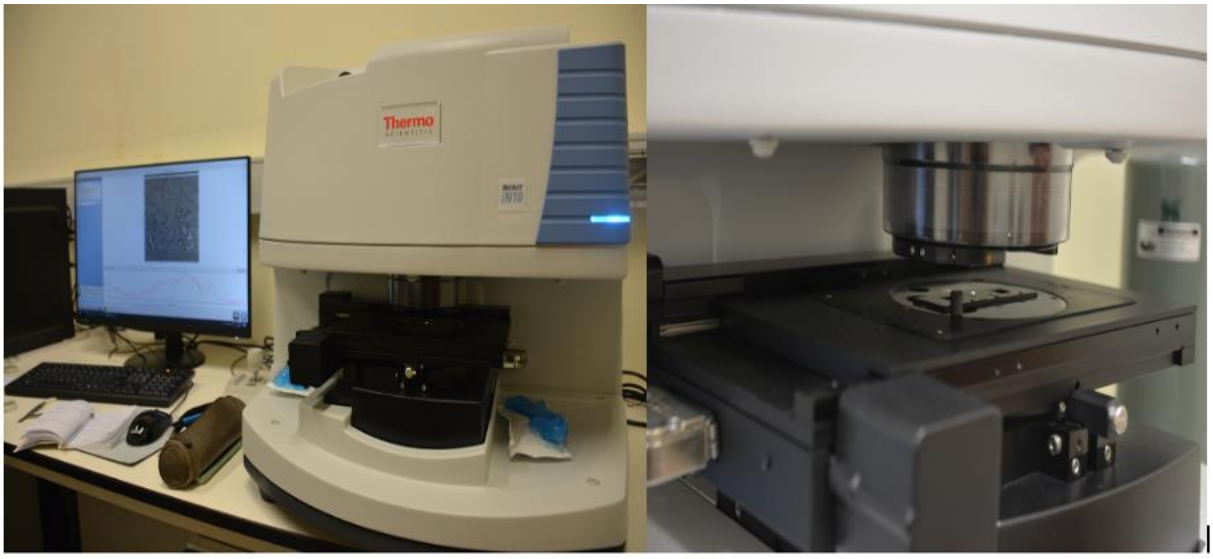

Figure 7. Nicolet iN10 MX -FTIR microscope used for the analysis of microplastic polymers.

Table 1. Principal spectral absorption peak positions (cm^{-1}) of the functional groups characterizing PET/BPET polymers, according to the current literatures.

Peak range (cm^{-1})	**Functional group**	**References**
3300	ν(O-H) amyl	Borchani, et al., 2015
2920-2924	Asymmetric -CH_2 Stretching	Miyake 1959; Jung, et al., 2018
1710-1740	Stretching - C=O (ketones)	Miyake, 1959 ;Cole, et al., 1994; Cole, et al., 2002; Donelli, et al., 2010; Djebara, et al., 2012; Chen, et al., 2015; Ioakeimidis, et al., 2016; Jung, et al., 2018; Mecozzi & Nisini, 2019; Denaro, et al., 2020
1647 - 1654	C=O mode of carboxylic acids	Socrates, 1994
1408 - 1470	Bending -CH2, Parasubstituted benzene ring, ring C-H in plane bending	Miyake, 1959; Cole, et al., 1994 ; Cole, et al.,2002; Donelli, et al., 2010;Djebara, et al.,2012;Chen, et al., 2015;Mecozzi & Nisini, 2019 ;Denaro, et al., 2020
1368-1371	Gauche wagging band-CH2, amorphous phase	Miyake, 1959; Bahl, et al., 1974; Cole, et al., 1994; Cole, et al., 2002; Donelli, et al.,

		2010; Djebara, et al., 2012; Chen, et al., 2015; Mecozzi & Nisini, 2019
1340 -1342	Trans wagging band -CH_2, Crystalline phase	Miyake, 1959; Bahl, et al., 1974; Cole, et al., 2002; Donelli, et al., 2010; (Djebara, et al.,2012; Chen, et al., 2015;Mecozzi & Nisini, 2019; Denaro, et al., 2020
1241- 1269	Asymmetric Stretch C-C-O group bonded to aromatic ring, C=O in-plane bending	Bahl, et al.,1974; Cole, et al., 2002;Donelli, et al., 2010; Djebara, et al., 2012; Chen, et al., 2015; Ioakeimidis, et al., 2016; Jung, et al., 2018; Mecozzi & Nisini, 2019; Denaro, et al., 2020
1094 –1120	Stretching C-O-C group	Miyake, 1959; Bahl, et al., 1974; Cole, et al., 2002; Donelli, et al.,2010;Djebara, et al., 2012; Ioakeimidis, et al., 2016; Jung, et al., 2018;Mecozzi & Nisini, 2019; Denaro, et al., 2020
1042-1045	Gauche C-O stretching, Gauche O-CH_2 stretching	Miyake, 1959; Cole, et al. 1994; Cole, et al., 2002; Donelli, et al., 2010; Djebara, et al., 2012; Chen, et al., 2015
1013-1024	Aromatic ring C-H in-plane bending, ring CCC bending, ring CC stretching, ν(C-O) amyl	Miyake, 1959; Cole, et al., 1994; Cole, et al., 2002; Donelli, et al., 2010; Djebara, et al., 2012; Chen, et al., 2015; Borchani, et al., 2015
971-978	Gauche bending oxy-methylene group, trans -C-O stretching	Miyake, 1959; Cole, et al., 1994; Cole, et al., 2002; Donelli, et al., 2010; Djebara, et al., 2012; Chen, et al., 2015; Mecozzi & Nisini, 2019
871 – 898	Trans bending oxy-methylene group (CH_2 rocking)	Miyake, 1959; Cole, et al., 1994; Cole, et al., 2002; Donelli, et al., 2010; Djebara, et

		al., 2012; Chen, et al., 2015; Ioakeimidis, et al., 2016; Mecozzi & Nisini, 2019
720-730	Aromatic C-H out of plane bending, C=O out-of-plane bending ring torsion	Miyake, 1959; (Cole, et al., 1994; Cole, et al., 2002; Donelli, et al., 2010; Djebara, et al., 2012; Chen, et al., 2015; Ioakeimidis, et al., 2016; Denaro, et al., 2020

2.5.3. Chemical Oxygen Demand (COD)

To determine if actual biodegradation (i.e. assimilation and mineralization of the plastic polymers; Lucas et al., 2008) process was taking place in our samples during the experiment, the amount of oxygen that is required to chemically oxidize MPs into their metabolic products was analysed (Shah, et al., 2008). Since the marine broth used in our experiments contained yeast as a carbon source, analyzing the release of CO_2 from our samples may not be an adequate technique to evaluate the biodegradation of MP films. Therefore, to avoid the interference of other carbon sources, we decided to measure the COD from the plastics particles themselves rather than from the marine broth containing the MP particles.

For this, at the beginning and at the end of each experiment, five MP particles were introduced into COD cuvette tests for photometric determination (HACH, Germany), as an alternative to as standard respirometric (Hoffmann, et al., 1997; Krzan, et al., 2006) and Sturm tests (Pagga, 1997), which are based on the consumption of oxygen and formation of carbon dioxide, respectively. The cuvettes used in our experiment contained a mixture of oxidizing reagents that were capable to degrade the MP particles, following the ISO 15705 protocol.

2.5.4. Scanning Electron Microscopy (SEM)

Scanning Electron Microscopy (SEM) has proven to provide a great depth and fine surface details of microplastics (Bin, et al., 2022). At the end of each experiment (after 90 and 45 days of incubation for communities and isolates, respectively) one MP from each treatment was subjected to Scanning Electron Microscopy (SEM) analysis. The images were acquired using a high-resolution SEM (Hitachi S3700, BRUKER, USA). Prior to image acquisition, MPs particles from each treatment (PET/BPET with and without the inoculum) were washed with a 2% (v/v) aqueous

sodium dodecyl sulfate (SDS) solution (Harshvardhan & Jha, 2013) for 4 hours at room temperature. Particles were rinsed afterwards with distilled water and ethanol (70%), followed with drying at 60°C for 10 minutes (Skariyachan, et al., 2018). Given that microplastics are non-conductive and due to the fact that charging effects will severely distort SEM images, especially for small objects in high magnification (Bin, et al., 2022), the MPs films were coated with gold nanoparticles before mounted on the microscope, and then visualized under varying magnifications.

2.5.5. Bacterial community/Isolates identification

DNA extraction

To identify the bacterial community and isolates after 90 and 45 days of incubation, respectively, DNA was extracted from the samples using the nzytech NZY Microbial gNDA Isolation (NZYTech, Lisbon Portugal), following the protocol provided by the manufacturer. This was performed to classify the bacteria to the lowest possible taxonomic level, using 16S rRNA gene sequences. To observe the possible variations in the bacterial community attached to the particles, as compared to those in the surrounding broth, DNA was extracted from both, the marine broth and from the MP particles from all the samples The quality and concentration of eluted DNA was determined by measuring the absorbance at 260 and 280 nm wavelengths using a NanoDrop spectrophotometer (NanoDrop One C, Thermo Scientific, United States).

In the case of bacterial communities, extracted DNA was sent to the Integrated Microbiome Resource laboratory (Halifax, Nova Scotia, Canada) for PCR amplification and sequencing of the full 16S gene (PacBio Sequel), using the primers 27F (AGRGTTYGATYMTGGCTCAG) and 1492R (RGYTACCTTGTTACGACTT) (Paliy, et al., 2009). Conditions used are described in Comeau, et al. (2017). The PCR was weak or failed in the case of bacteria recovered from the MP particles, presumably because bacteria were not able to grow enough onto the particles. As a consequence, we were only able to compare those bacteria growing in the broth, either in the positive controls or the PET/BPET treatments inoculated with the consortium.

For the samples from the experiment with isolates, PCR amplification and Sanger sequencing was performed in our laboratory, as detailed below.

PCR Amplification

For PCR amplification of the bacterial 16S rRNA gene, the universal primers for prokaryotes, 8F (forward) (5′- AGA GTT TGATCC TGG CTC AG -3′) and 1492R (reverse) (5′- GGT TAC CTT GTTACG ACT T-3′), were used. The reaction mixture was composed of 2 µL of DNA (at concentration 5 to 50 ng/µL), 10 µL of Supreme NZYTaq 2× Green Master Mix (Nzytech, Portugal), 0.5 µL of each primer (at 10 µM), and 7 µL of sterilized Mili-Q water, being the final reaction volume of 20 mL. The PCR amplification was accomplished in a thermocycler (2720 Thermal Cycler, Applied Biosystems, Foster City, USA) under the following conditions: an initial denaturation step of 95 °C for 5 min, followed by 35 cycles 94 °C for 30s (denaturation), 57 °C for 30s (primer annealing), 72 °C for 90s (primer elongation), and a final elongation for 7 min at 72 °C.

The amplified PCR products were run by electrophoresis in 1% (w/v) agarose gels in a 1× TAE buffer (AMRESCO, Solon, USA) solution. DNA was stained by adding 5 µL/L of GreenSafeÒ Premium (NZYTech, Lisbon Portugal) to the gels, and the electrophoresis was accomplished with 100 V per cm of gel length during 1h. The resulting gel was examined in a UV transilluminator (Biorad Universal Hood II Gel Doc System, UK) for visualization of the DNA fragment bands.

DNA Sequencing

The sequencing was performed as described by Palma, et al. (2021). The amplification of the 16S rRNA generated a PCR product of 1180 – 1200 bp. The sequencing reaction of the purified PCR product was accomplished by the Sanger method with primers 8F/1492R, in a BigDye Terminator Cycle sequencing v3.1 kit (Applied Biosystems, USA). A labelling dye for each of the nucleotides was used. The POP-7 polymer (Applied Biosystems, USA) was used as a separation matrix to perform DNA sequencing and fragment analysis in a Genetic Analysis 3130xl sequencer (Applied Biosystems, USA). The results were obtained by Sequencing Genetic Analysis Software, provided by CCMAR's Molecular Biology Platform.

Quality control of the sequence reads were done using the Geneious software (https://www.geneious.com). Both forward and reverse sequences from each sample were trimmed to remove unclear nucleotides, and clean sequences were used for pairwise alignment. The determination of taxonomic identity was carried by Blast search of Gene Bank database of NCBI

(https://blast.ncbi.nlm.nih.gov/). The sequences from the GenBank that showed higher similarity with ours were considered as potential genus/species present in the isolates. Then both sequences resulted in the current study and those downloaded from the GenBank were aligned using MAFFT v. 7 (http://mafft.cbrc.jp/alignment/server/) and manually adjusted using AliView (Larsson, 2007). Ambiguously aligned regions were excluded from the analyses. The data matrix use for phylogenetic analyses contained 1350 unambiguously aligned sites. The alignments were based on the nucleotide sequences.

The optimal model of DNA evolution for the analysis was obtained using the Akaike Information Criterion as implemented in MrModeltest 2.3 (Nylander, 2004). The GTR+I + G model was employed across sites. Bayesian Inference was conducted with MrBayes 3.2.6, and branch support was estimated by Posterior Probability (PP) (Ronquist & Huelsenbeck, 2003). Four Markov chains were run for 2 runs from random starting trees for 10 million generations, trees were sampled every 100 generations and 25% were discarded as burn-in. Maximum likelihood estimates were carried out by RAxML v.8.2.10 using the GTR +G + I model of site substitution (Stamatakis, 2014). The branch support was obtained by maximum likelihood bootstrapping (MLbs) of 1000 replicates (Hillis & Bull, 1993). Bayesian PPs ≥ 0.95 (Alfaro, et al., 2003), and MLb $\geq 70\%$ were considered to be significant.

2.6. Statistical Analysis

Shapiro-Wilk was performed for the variables under study, to evaluate whether data came from a normal distribution. Since this was not the case for most of the data ($p < 0.05$), the effect of marine bacterial community I18 on MPs degradation was evaluated by means of non-parametric tests using stata version 15 (STATA Corp Inc., TX, USA).The Wilcoxon signed-rank test was performed for the biodegradation experiments to look for differences between the samples containing the bacterial community I18 and the negative controls (samples containing MPs but without any bacterial inoculum). Equally, we looked for statistical differences through the experiment (i.e., between the different sampling times). The test was performed for PET and BPET MP spectral peaks recorded by FTIR-ATR (Table 2), for optical density and the pH measurements. Same statistical tests were also performed for the bacteria isolates.

3. RESULTS AND DISCUSSION

3.1. FTIR-ATR spectra of PET/BPET MP (communities and isolates)

FTIR-ATR spectra results of both PET and BPET MPs for both bacteria communities and the isolates measured at the end of the incubation periods are shown in Figures 8 ,9, 10 and 11, and compared to the spectra of both polymers measured before the start of the experiments. Eight major absorption peaks were identified and used for the characterization of PET/BPET, as shown in Table 2 below. These bands are similar to those which have been frequently used to characterize the degradation or changes in the functional groups in the PET/BPET chain (Denaro, et al., 2020), as well as to discriminate PET and BPET because some of these spectral peaks also have been used to describe the crystalline and the amorphous characteristics of PET/BPET (Atkinson, et al., 2000; Mecozzi & Nisini, 2019). Peak at 3311 cm^{-1} was observed only on BPET while peaks at 1473 and 1339 cm^{-1} were only observed on the PET samples. Peaks at 1473, 1339, 1244-1269, 1097-1103, 970 & 724-729 are markers of the crystalline structure of PET while those at 1372 & 872-874 characterize amorphous conformation (Donelli, et al., 2010, Mecozzi & Nisini, 2019).

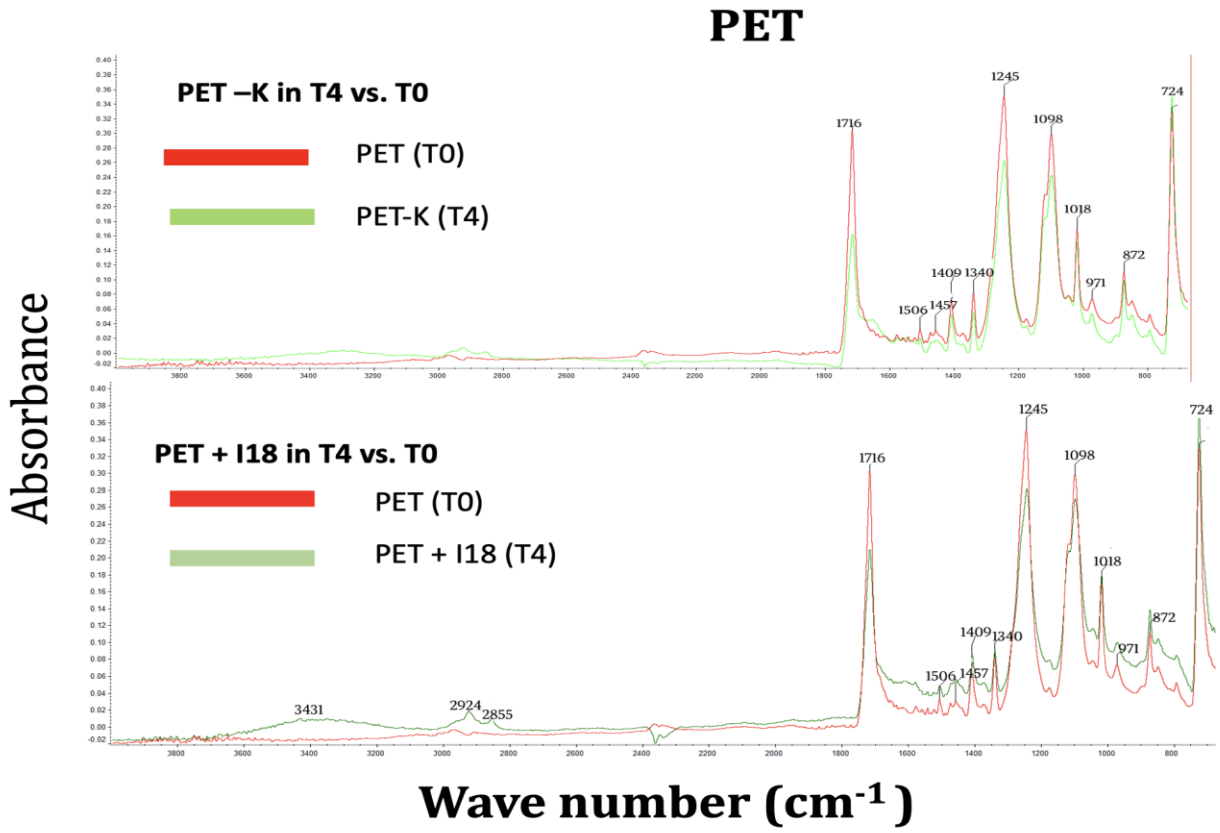

Figure 8. Spectral profile of PET microplastics, as determined by FTIR-ATR. The plot shows the results of the spectrum of the negative control (PET-K, on the top) and the sample with the bacterial consortium (PET +I18, at the bottom) at the end of the experiment (T4), superimposed to the spectrum of PET microplastics at the beginning of the experiment (T0).

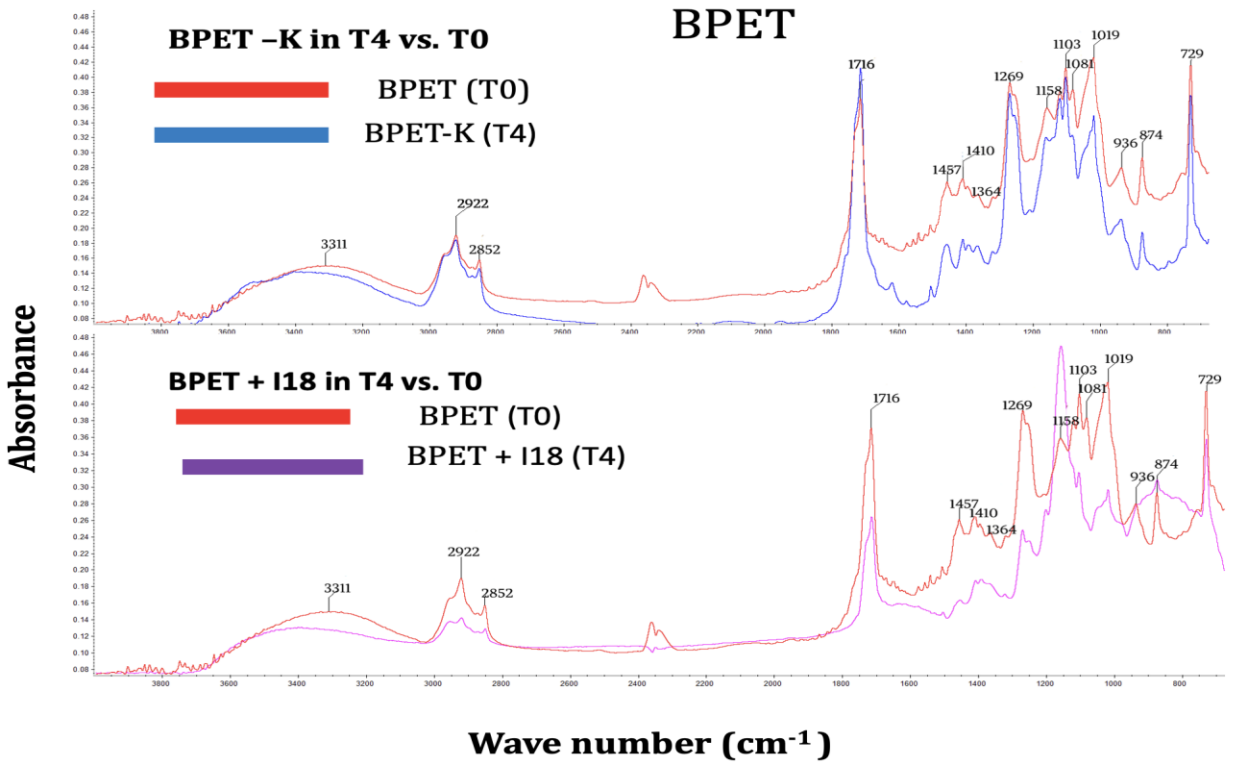

Figure 9. Spectral profile of BPET microplastics, as determined by FTIR-ATR. The plot shows the results of the spectra spectrum of the negative control (BPET-K, on the top) and the sample with the bacterial consortium (BPET +I18, at the bottom) at the end of the experiment (T4), superimposed to the spectrum of BPET microplastics at the beginning of the experiment (T0).

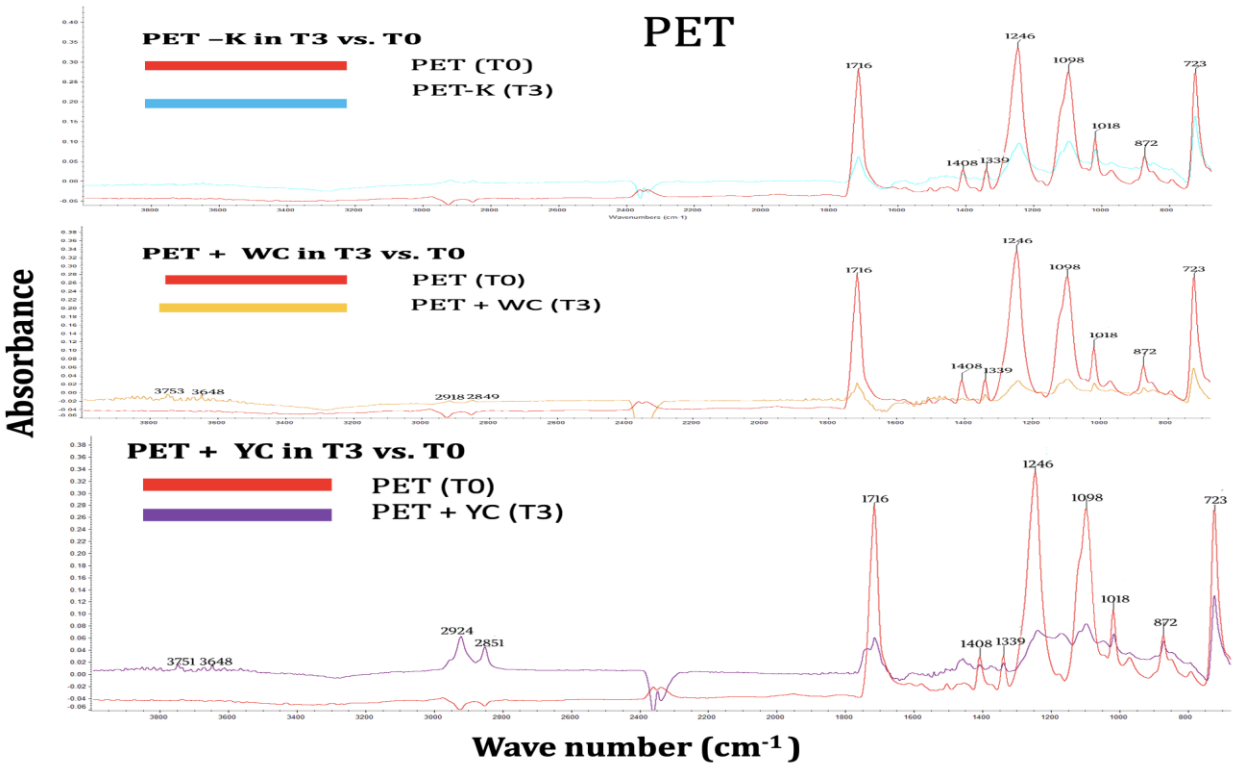

Figure 10. Spectral profile of PET microplastics, as determined by ATR-FTIR. The plot shows the results of the spectra spectrum of the negative control (PET-K, on the top), a sample inoculated with the bacterial isolate WC (PET+WC, in the middle) and a sample inoculated with the bacterial isolate YC (PET+YC, bottom) at the end of the experiment (T3), superimposed to the spectrum of PET microplastics before the incubation (T0).

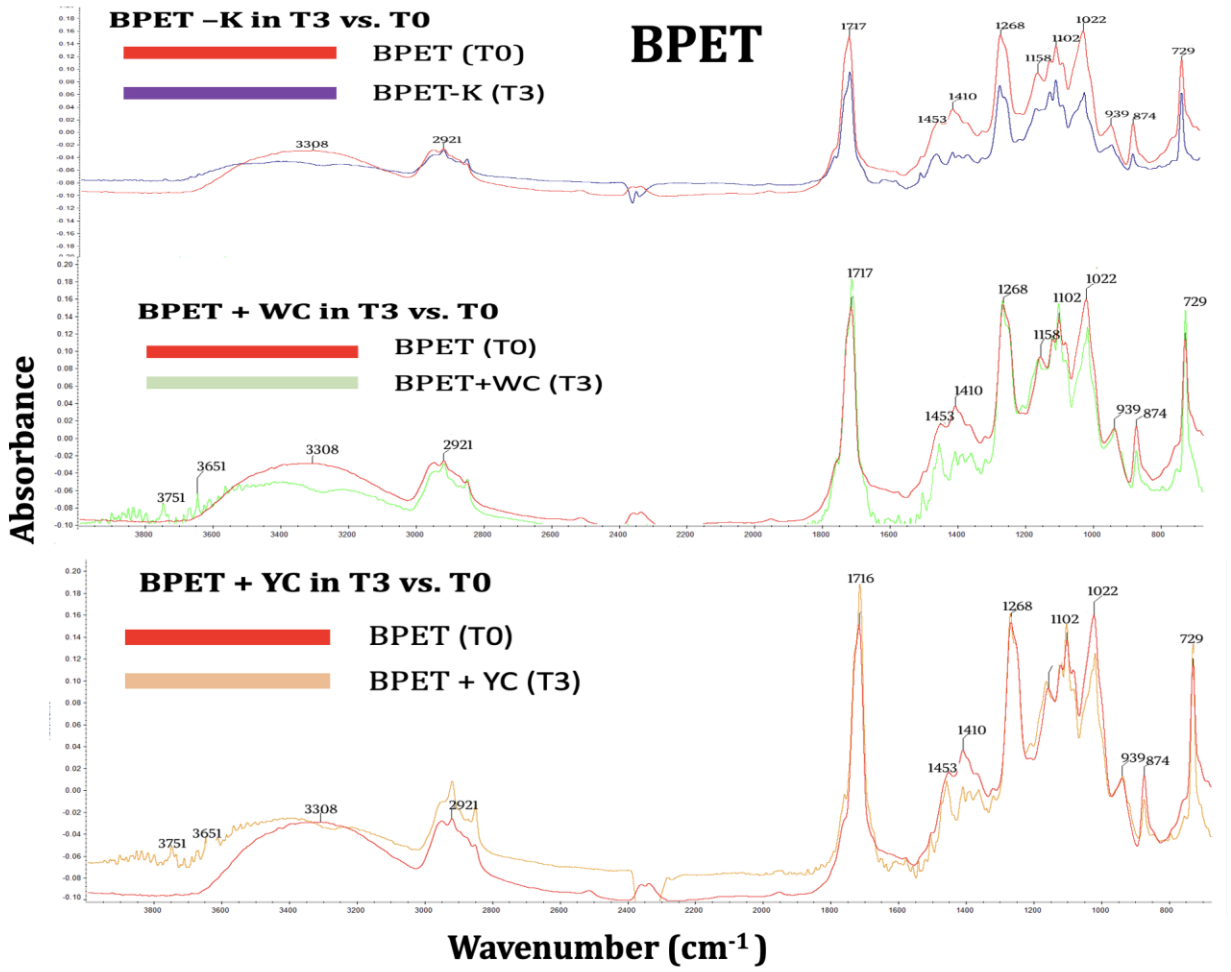

Figure 11. Spectral profile of BPET microplastics, as determined by ATR-FTIR. The plot shows the results of the spectra spectrum of the negative control (BPET-K, on the top), a sample inoculated with the bacterial isolate WC (BPET+WC, in the middle) and a sample inoculated with the bacterial isolate YC (BPET+YC, bottom) at the end of the experiment (T3), superimposed to the spectrum of PET microplastics before the incubation (T0).

3.1.1. PET biodegradation with Bacteria Community #I18 and Isolates WC and YC

For the PET particles treated with the bacteria communities Community #I18 and Isolates WC and YC, the spectra peak at 3431 cm^{-1} corresponds to the carboxylic acid and alcohol functional groups (R-OH stretching, 3000-3500 cm^{-1}) (Sammon et al., 2000). The formation of this new peak might be attributed to the creation of an additional ester (C=O, C-O), carboxyl (C=O, C-O, O-H), or alcohol (- OH) bond that is created in the PET particles as they degrade (Roberts, et al., 2020).

The statitiscal analysis showed significant differences between treatments for peaks observed in the footprint region (Tables 2 and 3). More specifically, it was observed in the absorbance peaks at positions 1473, 1339, 1238, 1097, 1018-1022, 871-874 and 723 -729 cm^{-1}. Significant decrease in the absorbance peaks at positions 2851 and 1647 cm^{-1} was also observed in PET particles inoculated with isolates WC and YC (Table 3).The significant decrease in the intensity of the carbonyl stretching band (1716 cm^{-1}) observed in the PET particles treated with the inoculum #I18 as the function of time (Table 2) further confirms the involvement of the ester carbonyl group in the biocatalytic attack (Donelli, et al., 2010; Sriromreun, et al., 2013).

The appearance of new peaks, significant increase and decrease in intensities of absorbance peaks observed in the PET MP could be due to PET MP degradation by the bacterial communities #I18 and isolates WC and YC leading to the formation of additional ester (C=O, C-O), carboxyl (C=O, C-O, O-H), or alcohol (C-O, OH) bonds in the PET MP (Roberts, et al., 2020; Zannat, 2021), where the appearance or alteration of those bonds tends to change peak intensities at those absorbance positions (Socrates, 1994; Sriromreun, et al., 2013). Similar results have been reported in previous PET degradation studies (Ioakeimidis, et al., 2016; Janczak, et al., 2020; Roberts, et al., 2020).

These results suggest that, bacteria community #I18 and isolates WC and YC had induced the hydrolysis reaction of PET particles, including the formation of carboxylic acid end groups, leading to the cleavage of PET polymer ester bonds (Sammon, et al., 2000; Gao & Sun, 2021). In addition to that, the observed significant decrease in the intensity of some spectral peaks in PET samples treated with bacteria community #I18 and isolates WC and YC are also an indication of either the decrease of the concentration of the original bond and/or the change in the chemical environment of the bond (Djebara, et al., 2012). The observed decreases in the carbonyl bond is expected during PET degradation, as C=O and C-O bonds are broken during ester cleavage (Roberts, et al., 2020). Similar spectra changes have been reported for degraded PET samples in the marine habitat (Ioakeimidis, et al., 2016). Furthermore, similar results have been reported in a study that lasted up to 6 month (Gao & Sun, 2021).

3.1.2 BPET biodegradation with Bacteria Community #I18 Isolates WC and YC

For the BPET samples treated with bacteria inoculum #I18 and isolates WC and YC, the most significant differences were observed at the fingerprint region, i.e., from 1500 to 500 cm^{-1} and more specifically, it was observed the decrease in the absorbance of peaks at positions 1473, 1339, 1238, 1097, 1019- 1022 and 723 -729 cm^{-1} (Tables 4 and 5), which are attributed to different functional groups listed in Table 1. For the BPET particles inoculated with inoculum #I18 , the decrease in intensity of the peak at 1716 - 1717cm^{-1} was also observed.This decrease mighty be due to the vibration of the ester group (Ward & Wilding, 1977; Cole, et al., 2002; Donelli, et al., 2010). Sriromreun, at al., (2013), reported the similar decreased intensity of C=O streching mode of the aromatic 1716 cm^{-1} in the degradable aliphatic/aromatic copolyester. An increase in intensity as a function of time is also observed in the 1685 cm^{-1} band (Table 4), which is assigned to C=O mode of carboxylic acids (Socrates, 1994), confirming that COOH end groups are generated as a result from hydrolysis of the copolymers (Sriromreun, et al., 2013) . The shifts in these bands could possibly indicate that the polymer is being degraded by the selected bacterial consortium #I18 and isolates WC and YC (Fernández de Villalobos, et al., 2022).

The bands at 3311 and 1018-1020 cm^{-1} observed in BPET corresponded to O-H and C-O stretching vibrations of amylose and amylopectin, the two main components of starch (Borchani, et al., 2015). The band at 3311 was also reported to correspond to the O-H stretching of the diethylene glycol end group (Holland & Hay, 2002). The existence of these two bands and others at peak positions 872-874, 936, 1103, 1364 and 1455-1457 cm^{-1} which are attributed to different functional groups listed in Table 1, in the FTIR-ATR spectrum of BPET, confirms the presence of biobased segments in the PET copolymer structure (Sriromreun, at al., 2013; Mecozzi & Nisini, 2019). Furthermore, for the BPET particles treated with the bacterial community #I18, spectral peaks at positions at 1018 - 1020 cm^{-1} bands, had a relatively significantly low intensity compared to the control (Table 4). Appearance of the new peaks and consequently changes in the intensities of peaks is an indication that BPET MP particles were degraded by the bacterial community #I18, isolates WC and YC. Similar results were reported in previous studies (Sriromreun, et al., 2013; Fernández de Villalobos, et al., 2022).

However, to date, there is a lack of information regarding the changes in the functional groups of PET as the result of microbial biodegradation, especially for biobased PET, which is the polymer of interest in this study. Our results could in this sense pave the way for further interpretation of changes in the functional groups of PET due to biodegradation and for the development of standard methods that can be applied to the biobased PET, which are essential in property assessment and determination of their potential applications.

Table 2. Results of non-parametric Wilcoxon-test for the different variables measured in the samples containing PET MPs (K and samples containing the bacterial inoculum #I18) at the 95% level of statistical significance. *p<0.05; **p<0.01; ***p<0.001; n.s.: non-significant (p>0,05).

Measured variable	Assay (K vs.I18)	Incubation time (T1-T4)
Optical density	n.s.	T1 > T4*
pH	n.s	T1 > T3*
		T1 > T4*
3728/33 cm^{-1}	n.s	T1 < T2**
		T2 > T3**
		T2 > T4**
		T3 > T4**
3649 cm^{-1}	n.s.	T1 < T2*
		T1 < T4**
		T3 < T4*
3291/93 cm^{-1}	n.s.	n.s.
2919/24 cm^{-1}	n.s.	T1 < T4**
		T2 < T4**
2851 cm^{-1}	n.s.	T1 < T4**
		T3 < T4*
	K > I18**	T1 >T2***

1710/16 cm^{-1}		T1 > T4***
		T2 < T3***
		T2 < T4*
		T3 > T4***
1647/54 cm^{-1}	n.s.	T1 < T2*
		T2 > T3*
1470/74 cm^{-1}	K > I18**	n.s.
1453/57 cm^{-1}	n.s.	T1 > T2***
		T1 > T4*
		T2 < T3***
		T2 < T4***
1408/10 cm^{-1}	n.s.	T1 > T2***
		T1> T4**
		T2 > T3***
		T2 < T4**
		T3 < T4*
1339/72 cm^{-1}	K> I18*	T1 > T2***
		T1 > T4***
		T2 < T3**
		T2 < T4***
1238/70 cm^{-1}	K > I18**	T1> T2***
		T1 < T3*
		T1> T4***
		T2 < T3***
		T2 < T4**
		T3>T4***
	K > I18**	T1 > T2**

1097/1100 cm^{-1}		T1 > T4***
		T2 < T3**
		T3 > T4***
1016/20	K > I18**	T1 > T2***
		T1> T4**
		T2 < T3**
		T3 > T4**
933/72 cm^{-1}	n.s.	T1 > T2**
		T1 > T4***
		T2 <T3**
		T2 < T4**
		T3 > T4*
871/74 cm^{-1}	n.s.	T1 > T3*
		T1 > T4***
		T2 > T4**
		T3 > T4**
723/29 cm^{-1}	K > I18**	T1>T2***
		T1 > T4**
		T2< T3***
		T3 > T4**

Table 3. Results of non-parametric Wilcoxon-test for the different variables measured in the PET samples (K and samples containing the bacterial inoculum WC) at the 95% level of statistical significance. *p<0.05; **p<0.01; ***p<0.001; n.s.: non-significant (p>0,05).

Measured variable	**K vs PET + WC**	**Incubation time (T1-T3)**
Optical density	K < PET +WC***	T1 < T2*
		T1< T3*
pH	K > PET +WC***	T1 > T3*
		T2 > T3*
3728/33 cm $^{-1}$	K < PET +WC **	T1 < T2**
		T1 > T3*
3649 cm $^{-1}$	K < PET +WC **	T1 > T2***
		T1 > T3*
		T2 < T3**
3291/93 cm $^{-1}$	n.s.	n.s.
2919/24 cm $^{-1}$	K < PET +WC *	T1 > T2**
		T2 < T3**
2851 cm $^{-1}$	K < PET +WC *	T1 > T2**
		T2 < T3**
1710/16 cm $^{-1}$	n.s.	n.s.
1647/54 cm $^{-1}$	K > PET +WC *	n.s.
1470/74 cm $^{-1}$	K < PET +WC ***	T1 > T2**
		T1 > T3**
1453/57 cm $^{-1}$	K < PET +WC ***	T1 < T2*
1408/10 cm $^{-1}$	n.s.	n.s.
1339/72 cm $^{-1}$	K < PET +WC **	n.s.
1238/70 cm $^{-1}$	n.s.	T2 > T3**
1097/1100 cm $^{-1}$	n.s.	T2 > T3**
1016/20 cm $^{-1}$	n.s.	T2 > T3*
933/72 cm $^{-1}$	K < PET +WC **	n.s.

871/74 cm $^{-1}$	K < PET +WC *	T2 > T3*
723/29 cm $^{-1}$	n.s.	T2 > T3**

Table 4. Results of non-parametric Wilcoxon-test for the different variables measured in the PET samples (K and samples containing the bacterial inoculum YC) at the 95% level of statistical significance. *p<0.05; **p<0.01; ***p<0.001; n.s.: non-significant (p>0,05).

Measured variable	K vs PET + YC	Incubation time (T1-T3)
Optical density	K < PET + YC ***	T1 < T2*
		T1 < T3*
pH	K > PET + YC ***	T1 > T2*
		T1> T3*
		T2 > T3*
3728/33 cm $^{-1}$	K < PET + YC ***	T1 > T2**
3649 cm $^{-1}$	K < PET + YC **	T1 < T2**
		T2 < T3**
3291/93 cm $^{-1}$	n.s.	n.s.
2919/24 cm $^{-1}$	n.s.	T1 > T2*
		T2 < T3**
2851 cm $^{-1}$	n.s.	T1 > T2*
		T2 < T3**
1710/16 cm $^{-1}$	n.s.	n.s.
1647/54 cm $^{-1}$	n.s.	n.s.
1470/74 cm $^{-1}$	K < PET + YC ***	T1 > T2*
1453/57 cm $^{-1}$	K < PET + YC ***	n.s.
1408/10 cm $^{-1}$	n.s.	n.s.
1339/72 cm $^{-1}$	K < PET + YC *	n.s.
1238/70 cm $^{-1}$	n.s.	n.s.
1097/1100 cm $^{-1}$	n.s.	n.s.

1016/20 cm $^{-1}$	n.s.	n.s.
933/72 cm $^{-1}$	K< PET + YC **	n.s.
871/74 cm $^{-1}$	K < PET + YC *	n.s.
723/29 cm $^{-1}$	n.s.	n.s.

Table 5. Results of non-parametric Wilcoxon-test for the different variables measured in the samples containing BPET MPs (K and samples containing the bacterial inoculum #I18) at the 95% level of statistical significance. *p<0.05; **p<0.01; ***p<0.001; n.s.: non-significant (p>0,05).

Measured variable	K vs I18	Incubation time (T1-T4)
Optical density	n.s.	n.s.
pH	n.s.	T1 > T3*
		T1 > T4*
		T2 > T4*
3728/33 cm $^{-1}$	K< I18*	T1< T2*
		T2 > T3*
		T2> T4*
3649 cm $^{-1}$	n.s.	T1 < T2*
		T2 > T3*
3291/93 cm $^{-1}$	n.s.	n.s.
2919/24 cm $^{-1}$	K > I18**	T1 <T2**
		T1< T4***
		T2 > T3**
		T2 <T4*
		T3 < T4***
2851 cm $^{-1}$	K > I18*	T1< T2**
		T2 > T3**

1710/16 cm $^{-1}$	K> I18*	T1 > T2**
		T1 < T4*
		T2 < T3**
		T2 < T4**
		T3 < T4*
1647/54 cm $^{-1}$	n.s.	T1 > T3*
		T2 > T3***
		T2 > T4**
1470/74 cm $^{-1}$	K > I18**	n.s.
1453/57 cm $^{-1}$	K > I18**	T1 > T2**
		T1 > T3**
		T2 < T4*
		T3 < T4**
1408/10 cm $^{-1}$	n.s.	T1 vs T2-ns
		T2 < T4**
		T3 < T4**
1339/72 cm $^{-1}$	K > I18 ***	T1 > T4**
		T2 > T3**
		T2 > T4**
		T3 > T4**
1238/70 cm $^{-1}$	n.s.	T1 > T2***
		T1 > T3**
		T2 < T3**
		T2 < T4***
		T3 < T4**

1097/1100 cm $^{-1}$	n.s.	T1 > T3**
		T1 > T4**
		T2 < T3*
		T2 < T4*
		T3 < T4**
1016/20 cm $^{-1}$	K > I18***	T1 > T2***
		T1 > T3***
		T1 > T4**
		T2 < T4***
		T3 < T4***
933/72 cm $^{-1}$	K > I18*	T1 > T2*
		T1 > T3***
		T1 > T4***
		T2 > T3***
		T3 < T4**
871/74 cm $^{-1}$	n.s.	T1 > T3***
		T1 > T4*
		T2 > T3***
		T3 < T4***
723/29 cm $^{-1}$	K > I18**	T1 > T2***
		T1 > T3***
		T1 > T4*
		T2 > T3*
		T2 < T4***
		T3 < T4***

Table 6. Results of non-parametric Wilcoxon-test for the different variables measured in the BPET samples (K and samples containing the bacterial inoculum WC) at the 95% level of statistical significance. *p<0.05; **p<0.01; ***p<0.001; n.s.: non-significant (p>0,05).

Measured variable	K vs BPET + WC	Incubation time (T1-T3)
Optical density	K > BPET + WC **	T1 < T3*
pH	K < BPET + WC **	T1<T2*
3728/33 cm $^{-1}$	n.s.	n.s.
3649 cm $^{-1}$	n.s.	n.s.
3291/93 cm $^{-1}$	n.s.	n.s.
2919/24 cm $^{-1}$	n.s.	T1 <T3**
		T2 < T3**
2851 cm $^{-1}$	n.s.	T1 < T3**
		T2< T3**
1710/16 cm $^{-1}$	n.s.	T1 < T3**
1647/54 cm $^{-1}$	n.s.	n.s.
1470/74 cm $^{-1}$	n.s.	n.s.
1453/57 cm $^{-1}$	n.s.	n.s.
1408/10 cm $^{-1}$	n.s.	n.s.
1339/72 cm $^{-1}$	n.s.	n.s.
1238/70 cm $^{-1}$	n.s.	n.s.
1097/1100 cm $^{-1}$	n.s.	T1 > T2*
		T1 > T3*
1016/20 cm $^{-1}$	K > BPET + WC *	n.s.
933/72 cm $^{-1}$	n.s.	T1 > T3*
871/74 cm $^{-1}$	n.s.	T1 > T2*
		T1 > T3**
723/29 cm $^{-1}$	K > BPET + WC **	T1 > T3*
		T2 > T3**

Table 7. Results of non-parametric Wilcoxon-test for the different variables measured in the BPET samples (K and samples containing the bacterial inoculum YC) at the 95% level of statistical significance. *p<0.05; **p<0.01; ***p<0.001; n.s.: non-significant (p>0,05).

Measured variable	K vs BPET + YC	Incubation time (T1-T3)
Optical density	K < BPET + YC ***	T1 <T2*
		T1 < T3*
		T2 > T3*
pH	K> BPET + YC ***	T1 < T2*
		T1 < T3*
3728/33 cm $^{-1}$	n.s.	T1 < T3*
		T2< T3*
3649 cm $^{-1}$	n.s.	T1 <T3**
		T2 < T3**
3291/93 cm $^{-1}$	n.s.	n.s.
2919/24 cm $^{-1}$	n.s.	T1 > T2*
		T1 < T3**
		T2 < T3**
2851 cm $^{-1}$	n.s.	T1 >T2**
		T1 < T3**
		T2 < T3**
1710/16 cm $^{-1}$	n.s.	n.s.
1647/54 cm $^{-1}$	n.s.	T1 < T2*
1470/74 cm $^{-1}$	n.s.	n.s.
1453/57 cm $^{-1}$	n.s.	T1 > T2***
		T2 < T3**
1408/10 cm $^{-1}$	n.s.	T1 > T2**
		T1 > T3*

		T2 < T3**
1339/72 cm $^{-1}$	n.s.	T1 > T2*
		T2 < T3**
1238/70 cm $^{-1}$	n.s.	n.s.
1097/1100 cm $^{-1}$	n.s.	T1 > T2*
1016/20 cm $^{-1}$	K > BPET + YC *	T1 > T2**
		T1 > T3**
933/72 cm $^{-1}$	n.s.	T1 > T2***
		T1 > T3**
871/74 cm $^{-1}$	n.s.	T1 > T2***
		T1 > T3**
723/29 cm $^{-1}$	n.s.	T1 > T3**

3.2. Optical density and pH analysis

3.2.1. Optical density

Optical densities at 660 nm, as an indicator of the bacterial growth, showed a higher value in the microplastic samples containing bacteria inoculum, as compared to the negative controls (Figures 12 and 13) – as expected, indicating bacteria within community #I18 and isolates WC and YC are capable of utilizing MPs as carbon source. The bacteria community in the samples containing both PET and BPET MP showed an increase in growth from day 14 to day 90 (Figure 12). For the experiments with the isolates, a significant increase in growth was witnessed in the PET particles inoculated with isolate WC and PET and BPET MPs particles inoculated with isolate YC (Tables, 4, 3 and 7). For both PET/BPET particles inoculated with bacteria inoculum #I18 and PET and BPET MP particles inoculated with isolates WC and YC a higher growth rate was observed on day 28 and on day 45 for the PET sample inoculated with inoculum YC (Figures 12 and 13 and Tables 2, 3, 5, and 7) . This increase showed that the period was favourable for the interaction between the cell membrane of bacteria community #I18, isolates WC and YC and PET/BPET MPs, allowing for rapid metabolism (Auta, et al., 2017).

For the PET MP particles inoculated with bacteria community #I18, there was a slight decrease in the growth of the bacteria community from day 56 to day 90 (Figure 12). A sharp decrease in

growth was also observed in the BPET particles inoculated with bacteria isolates WC on day 45 (Figure 13) and this decrease was probably due to the lysis of cells, nutrient depletion or the presence of inhibitory products and microorganisms (fungi) in the culture media (Auta, et al., 2018). For BPET MP particles inoculated with the inoculum # I18, the growth decreased and this was probably due to the same previous reasons (Auta, et al., 2018). On day 56 and later, but then increased again at the end of the experiment (Figure 12). For the BPET MPs inoculated with the isolate WC, a significant decrease in growth was observed on day 45 (Figure 13 and Table 6). However, for both the BPET particles inoculated with bacteria inoculum #I18 and isolate YC this decrease in growth was not steep, and this may be ascribed to the potential of bacteria community I18 to influence the bonds of PET/BPET across time in order to maintain their metabolic activities, which include feeding and generation (Auta, et al., 2017). In any case, the statistical analysis did not show significant differences in bacterial growth between the negative controls and the samples containing PET and BPET particles treated with inoculum #I18 (Tables 2 and 5).

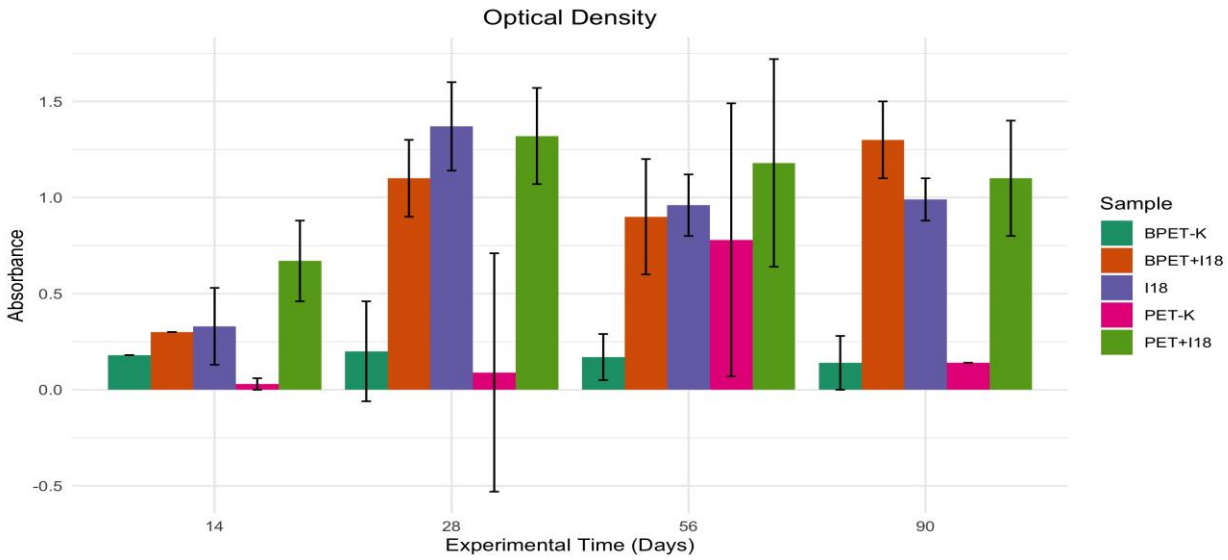

Figure 12. Results of the measurement of the optical density (at 660 nm) – as indicative of bacterial growth – throughout time in the different treatments. I18 and K stand for the positive (bacterial inoculum) and negative (microplastic particles, without bacteria) controls, respectively. Error bars represent the standard error from three replicates.

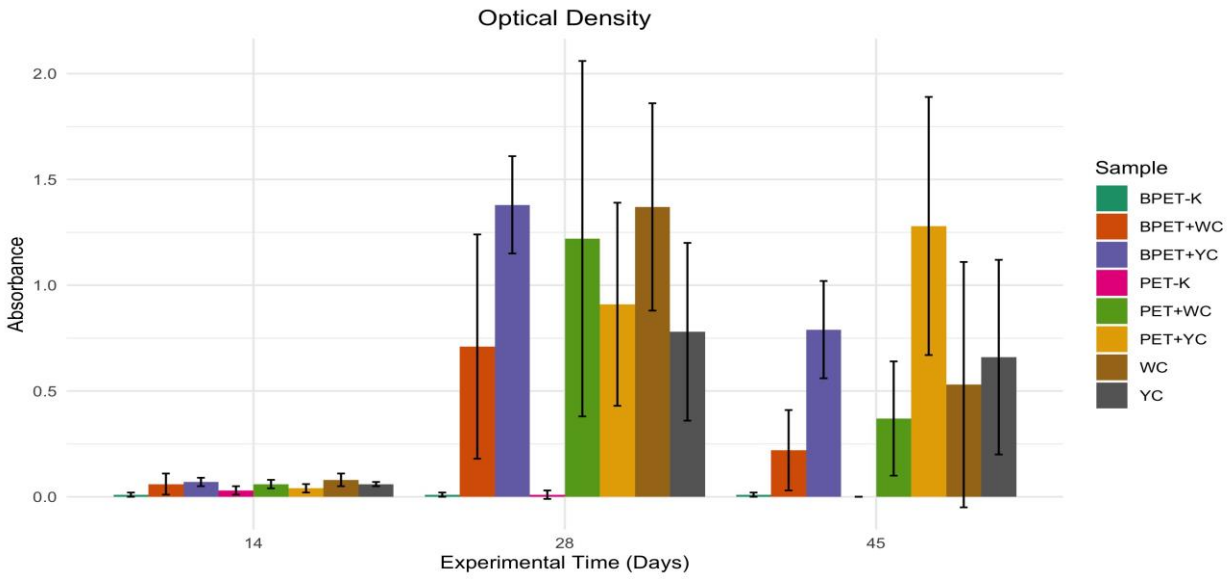

Figure 13. Results of the measurement of the optical density (at 660 nm) – as indicative of bacterial growth – throughout time in the different treatments. WC and YC corresponds to the bacterial isolates inoculated to the microplastic samples. K stands for the negative control (microplastic particles, without bacteria). Error bars represent the standard error from three replicates.

3.2.2. pH

Changes in the pH of PET/BPET MPs culture media during 90 days of incubation with the bacterial community I18 are shown in Figure 14. In general, the pH did not change that much through the incubation time, although in general, it decreased through time (Tables 2 and 5). The optimal pH for the growth of bacteria community I18 for both the PET and BPET samples was observed on day 28 when the pH was 8.8 ±013 and 8.54±0.22, respectively. The observed ranges are within the ranges (pH 5-10) required for the optimal growth of marine bacteria (Jung, et al., 2012). Under alkaline conditions, a larger amount of PET/BPET degradation products is produced, due to alkaline hydrolysis in which the hydroxide ion, which is a strong nucleophile, directly and irreversibly attacks the carbonyl group in the PET/BPET polymers, forming carboxylic acid which is neutralized and consumed by the bacteria (Brown, et al., 2011; Jones Jr. & Fleming, 2014), as a result, monomer formation is more rapid in alkaline conditions (Hirota, et al.,2020). Similar effects of pH were reported in the previous PET/BPET biodegradation studies (Xu, et al., 2011; Auta, et al., 2018; Hirota, et al., 2020; Fernández de Villalobos, et al.,2022). For Both PET, and BPET MP particles, pH values did not differ significantly among treatments according to the statistical test

performed (Tables 2 and 5). Similar results were reported in the previous study on biobased PET PET by marine bacteria, where, alkaline conditions seem to trigger the biodegradation process (Fernández de Villalobos, et.,2022) and on the effect of pH on the biodegradation of the biobased PET (biomax®), where the largest amount of biodegradation products was obtained in the alkaline conditions (Hirota, at al., 2020).

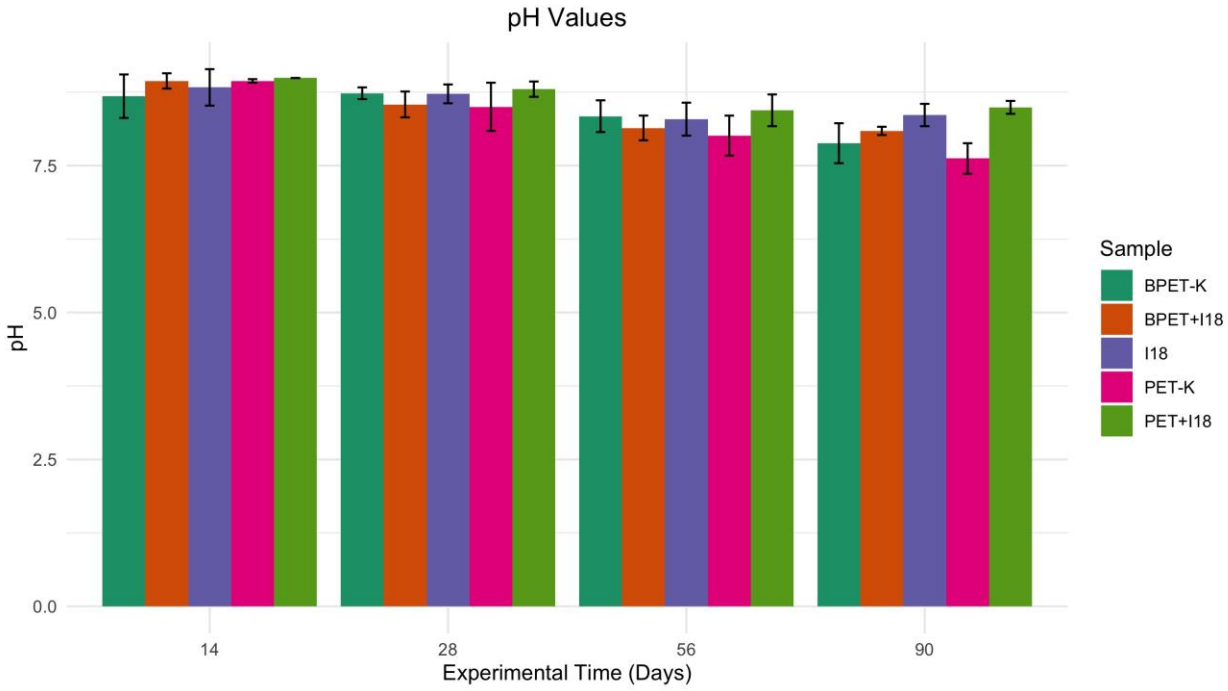

Figure 14. pH in the different treatments through incubation time. #I18 stands for the marine bacterial inoculate (positive control).

For the isolates, changes in the pH of PET/BPET MP culture media during 45 days of incubation with the bacteria isolates WC and YC, are shown in Figure 15. In the positive controls (WC and YC), the pH decrease was observed on day 14 for both WC and YC respectively. For the PET/BPET MP particles inoculated with both isolates, pH decreased significantly in the magnitude of nearly 0.5 (Figure 15 and Tables 3, 4, 6 and 7). The optimal pH for the growth of the PET and BPET MPs particles inoculated with the bacteria isolates WC and YC was observed on day 28 while for the PET particles inoculated with isolate YC on day 45. The observed decrease in pH

might be due to the formation of organic acids Glutaric acid (GA) during PET/BPET degradation by the isolates (Hirota, et al., 2020). Similar results have been reported in the previous biobased PET degradation study in which the largest amount of GA was obtained under acidic conditions (pH 3.0), this study also reported that biobased PET(biomax ®), can be hydrolyzed by both an exo-type mechanism under alkaline conditions and by an endo-type mechanism under acidic conditions (Hirota, et al., 2020).

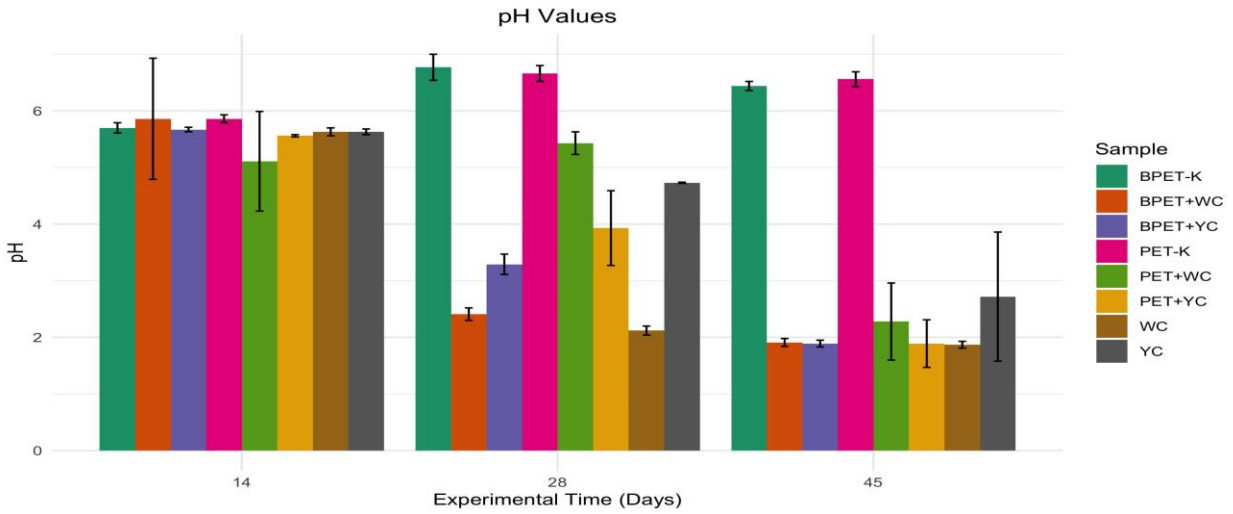

Figure 15. pH in the different treatments through incubation time. WC and YC stands for the marine bacterial isolates (positive controls).

3.3.COD and SEM Analysis

3.3.1 COD Analysis

For biodegradation experiment with bacterial communities, the negative control showed lower COD values than the experimental samples inoculated with bacteria. In addition, BPET microplastics containing the inoculum showed higher COD values than the PET particles with the same inoculum (Figure 16). This means that the BPET may require more oxygen to be degraded than the PET MPs. For the isolates, like for the bacteria inoculum treatments, the negative control samples showed less COD values than the samples containing the inoculum. However, unlike for bacteria communities, BPET microplastics containing the isolates had higher COD values than PET particles with the same isolates (Figure 17) indicating that, PET particles may require less oxygen to be degraded that the BPET MPs.

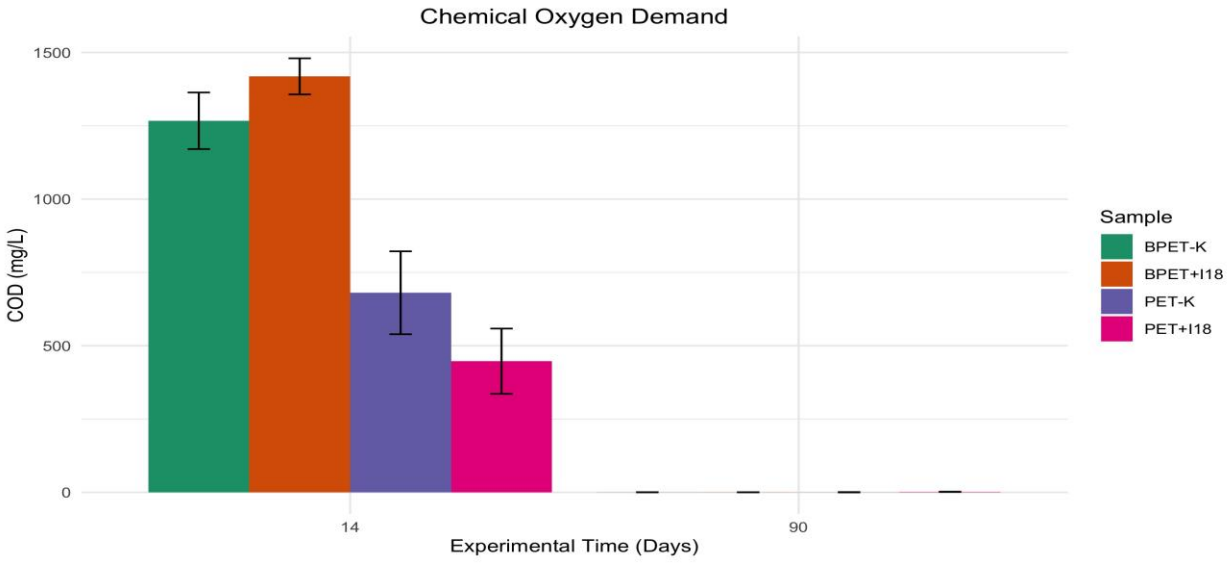

Figure 16. Representation of COD measured at the end of the experiment (after 90 days of incubation) for 5 PET and BPET particles. BPET/PET+I18 stand for the samples inoculated with marine bacteria (inoculum #I18), while BPET/PET-K stand for the negative controls.

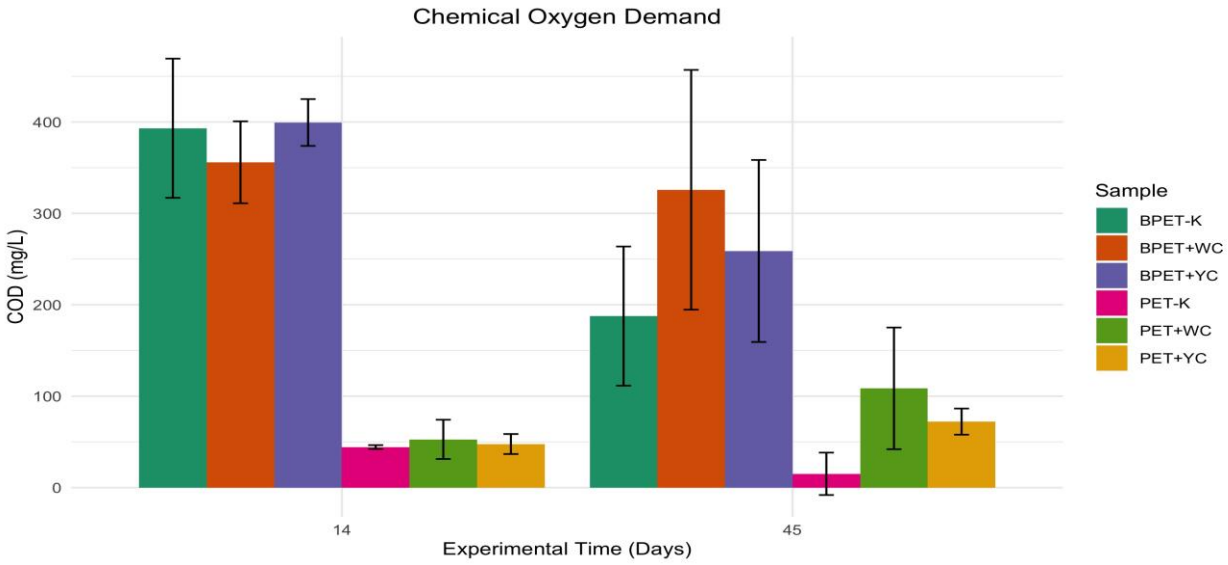

Figure 17. Representation of COD measured at the end of the experiment (after 45 days of incubation) for 5 PET and BPET particles. BPET/PET+WC/YC stand for the samples inoculated with marine bacteria isolates WC and YC, while BPET/PET-K stand for the negative contr

3.3.2. SEM analysis

Structural changes and adhesion of bacteria biofilms were observed in the surface of PET and BPET MPs particles exposed to bacterial consortia 18 (PET+I18 and BPET+I18), and to isolates (WC and YC), in comparison to the negative controls (PET-K and BPET-K). These changes include the presence of fractures, cavities, scratches and holes which were observed in the test samples (Figs. 18b and d; Figs. 19b and c; and Figs 20b and c), while the negative controls showed a smooth surface (Figs 18a and c; 19a and 20a).

Appearance of fractures, cavities, cracks, scratches and holes in the treated samples are likely due to the activity of the enzymes produced by the bacteria utilizing PET/BPET as their source of carbon (Ojha, et al., 2017; Alshehrei, 2017). PET/BPET MPs degradation was also supported by the formation and adhesion of bacteria biofilm in the surfaces of PET/BPET inoculated with the

bacteria (Kumar, et al., 2021). Biofilm formation has been described as a vital step for the colonization of microplastics by microorganisms and without them, plastic cannot be effectively degraded (Sivan, eat al., 2006). Furthermore, the results obtained in the present study are coherent to those obtained in the previous studies on PET/BPET polymers biodegration (Ioakeimidis, et al., 2016; Auta, et al., 2017 ; Denaro, et al., 2020 ; Gao & Sun, 2021).

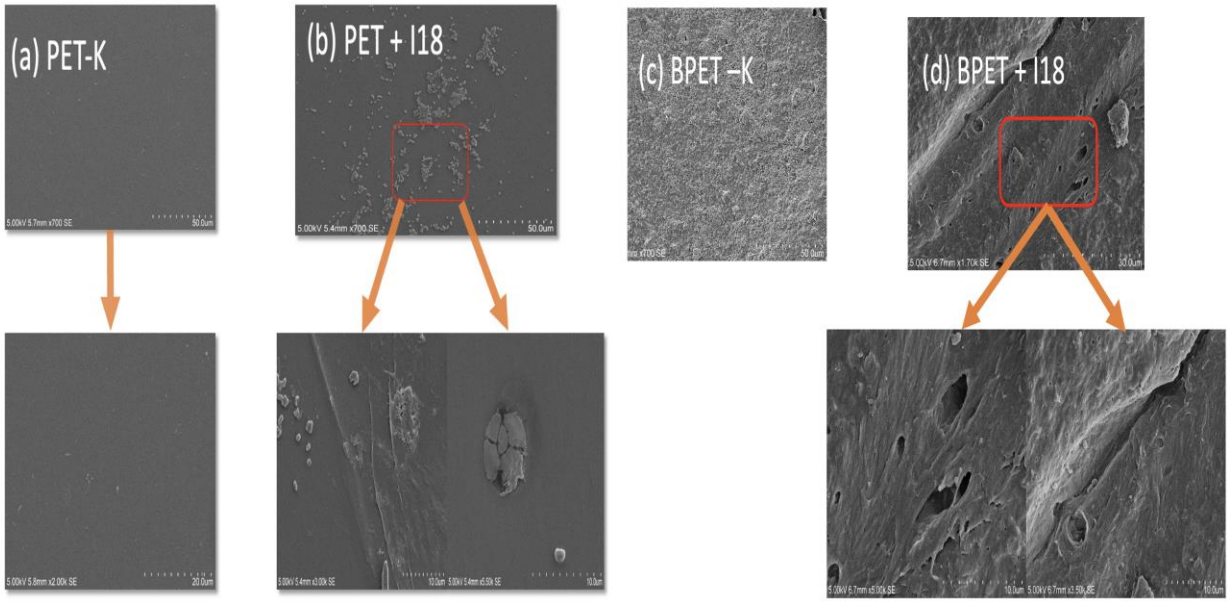

Figure 18a-d. Structural changes and adhesion of bacteria biofilms were observed in the surface of PET and BPET MPs particles exposed to bacterial consortia 18 (PET+I18 and BPET+I18), and to isolates (WC and YC), in comparison to the negative controls (PET-K and BPET-K). These changes include the presence of fractures, cavities and holes which were observed in the test samples (Figs. 18b and d; Figs. 19b and c; and Figs 20b and c), while the negative controls showed a smooth surface (Figs 18a and c;19a and 20a).

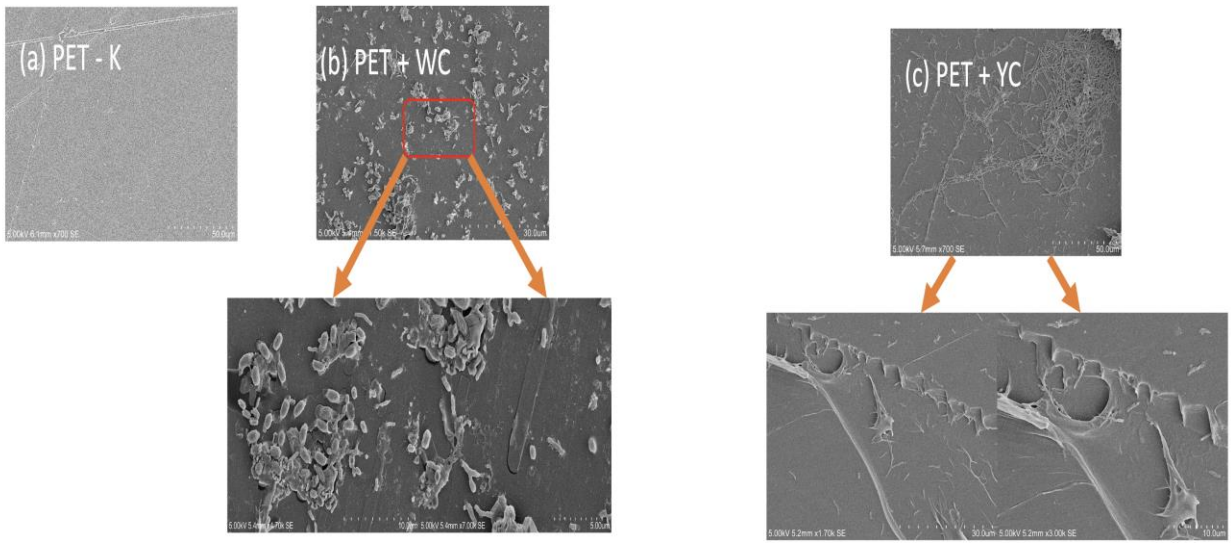

Figure 19. SEM micrographs of PET MP films after 45 days of incubation with the marine bacterial isolates (labelled as YC and WC), compared to the controls (labelled as K). (a) PET surface of a control particle depicting a smooth surface with no bacterial colonization on the surface; b) PET particle exhibiting structural changes with the formation of fractures and aggregation of bacteria after it was incubated with WC; c) PET MPs exhibiting structure changes with the formation of holes, fractures scratches and aggregation of bacterial biofilms after it was incubated with YC.

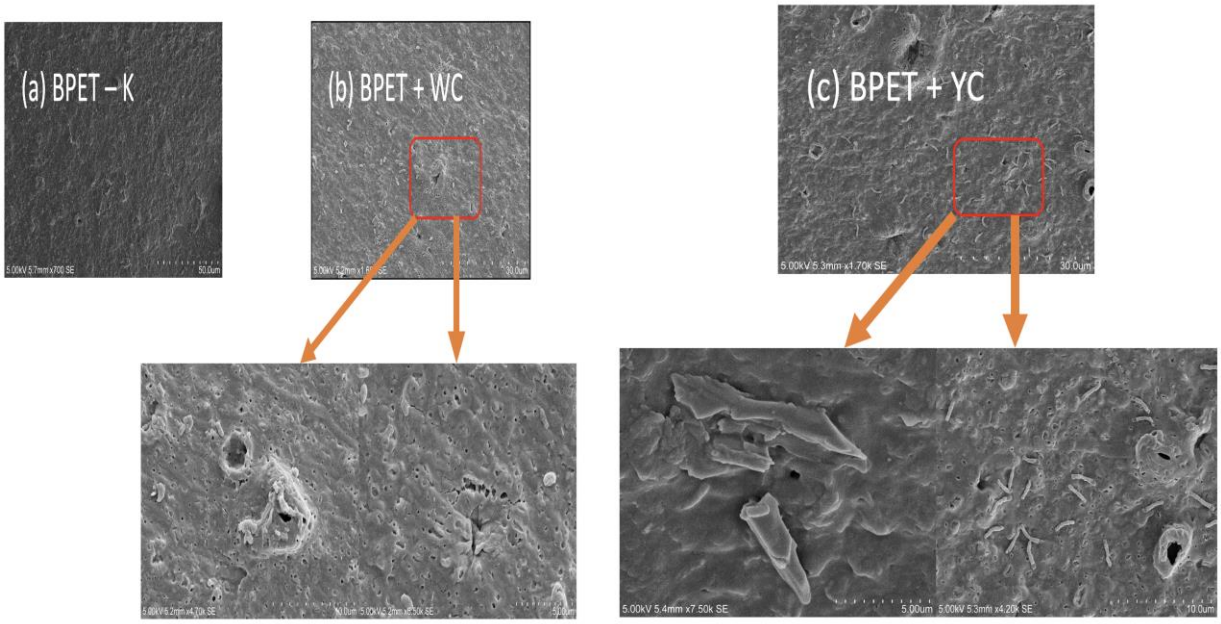

Figure 20. SEM micrographs of BPET MP films after 45 days of incubation with the marine bacterial isolates (labelled as YC and WC), compared to the controls (labelled as K). (a) BPET surface of a control particle depicting a smooth surface; b) BPET MP/particle exhibiting structure changes and aggregation of bacterial biofilms after it was incubated with WC; c) BPET MPs exhibiting structure changes with the formation of holes, cracks and aggregation of bacterial biofilms after it was incubated with YC.

3.4. DNA concentration and quality for bacterial community identification

3.4.1. DNA Concentration and Quality

The concentration of DNA extracted from the bacterial community adhered to the MP particles after 90 days of incubation ranged from 0.1 to 1.5 ng/µL . Similar results were reported in previous studies (Debeljak et al., 2017; Fernández de Villalobos, et al., 2022). The absorbance values at the ratio A280:A260 nm which indicate the quality of the eluted DNA, in most samples ranged from 0.13 to 7.54. The concentration of DNA extracted from the bacterial isolates (WC and YC) adhered to the MP particles after 45 days of incubation ranged from 0.4 to 3.4 ng/µL .These results were relatively higher compared to those obtained from bacterial community (#I18). Furthermore, the absorbance values at the ratio A280:A260 nm which indicate the quality of the eluted DNA were also higher compared to those obtained with the bacterial community.

3.4.2. Identification of bacteria

3.4.2.1. *Identification of the bacteria communities*

Classes, genera, and strains of bacteria identified from the bacteria community after 90 days of incubation are shown in Figures 21, 22 and 23. Most of the species found belonged to the class Bacilli (Figure. 21). The strains were assigned to 4 genera of class Bacilli (*Bacillus*) and one genera of class Alphaproteobacteria (*Paracoccus*) (Figure 22). The strains identified include those assigned to *Oceanobacillus oncorhynchi*, *Terribacillus goriens*, *Lysinibacillus chungkukjangi*, *Bacillus cohnii* and *Amia calva* (Figure. 23). The initial bacteria inoculum # I18 used in the experiment was only composed of members assigned to the genera *Arcobacter*, *Cutibacterium*, *Halodesulfovibrio*, *Marinobacter*, P*seudoalteromonas*, *Pseudomonas*, *Ruegeria*, *Shewanella*, *Tepidibacter* and *Vibrio* (Figure 1). However, after 90 days incubation period, a shift and increase in members assigned to the genus *Bacillus*, *Lysinibacillus*, *Mycobacterium*, *Oceanobacillus*, *Ornithinimicrobium*, *Paracoccus*, *Strepylococcus*, *Streptomyces* and *Teribacillus* was observed (Figures 23 and 25). These results suggest that the observed taxa were likely more resistant to BPET/PET MPs and could likely degrade or biofragment the PET/BPET MP and its metabolic products (Palma et al., 2021). The observed bacterial shift tends to occur when the community are exposed to, for example, different substrates (in this case, PET/BPET MP), since exposure to those substrates leads to an adaptation and or modification of the consortium (Moreira, et al., 2014). A similar mechanism of a shift in bacteria community during degradation was reported in the

previous study (Palma et al., 2021). The identified strains were similar to the ones that are native to marine habitats (Auta, et al., 2017). The strains belonging to the genera of class Alphaproteobacteria (*Paracoccus*) have also been reported to degrade biodegradable plastic (Denaro, et al., 2020). *Bacillus* spp., and Alphaproteobacteria have also previously been reported to be colonisers of plastics in the marine environment (Carson, et al., 2013; Oberbeckmann, et al., 2014). *Bacillus* has also been described as being efficient hydrocarbon-degrading bacteria (Yakimov, et al., 2007).

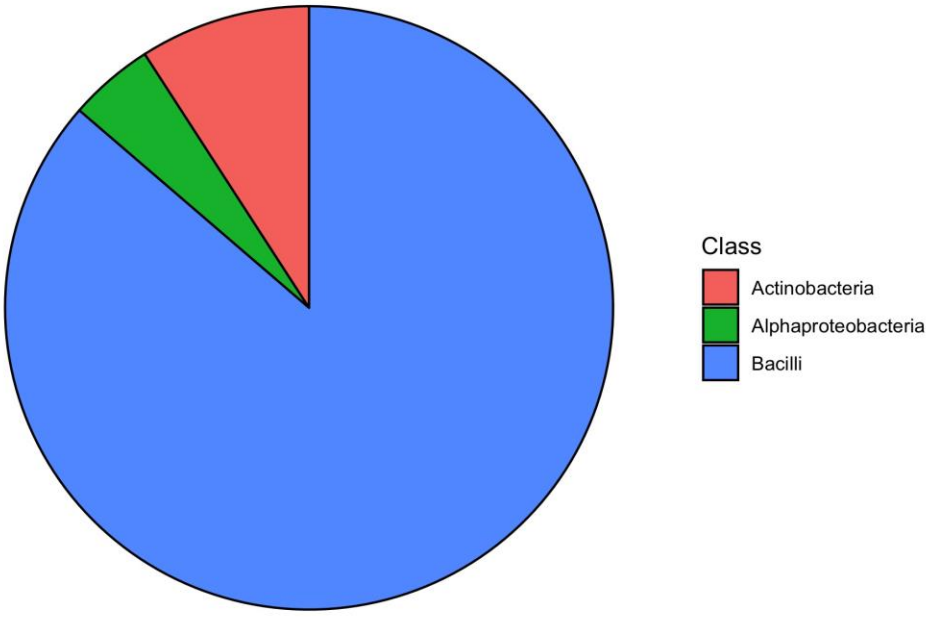

Figure 21. Relative abundance quantification of bacteria Community #I18 using 16S rRNA sequencing, following a 90-days incubation with both PET and BPET MP (Class)

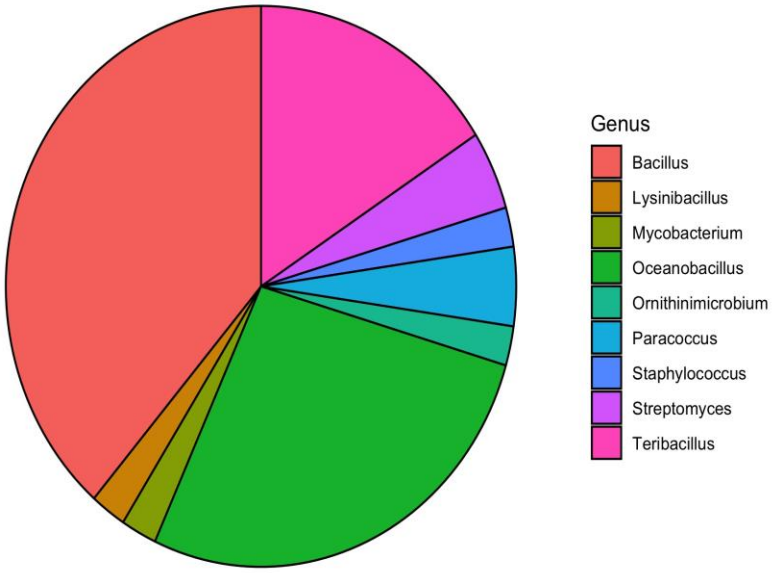

Figure 22. Relative abundance quantification of bacteria Community #I18 using 16S rRNA sequencing, following a 90-days incubation with both PET and BPET MP (genera).

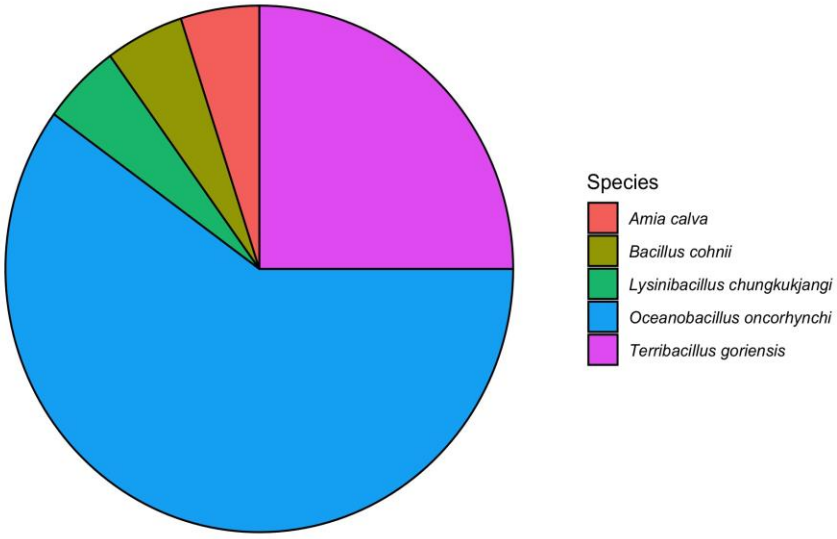

Figure 23. Relative abundance quantification of bacteria Community #I18 using 16S rRNA sequencing, following a 90-days incubation with both PET and BPET MPs (Species).

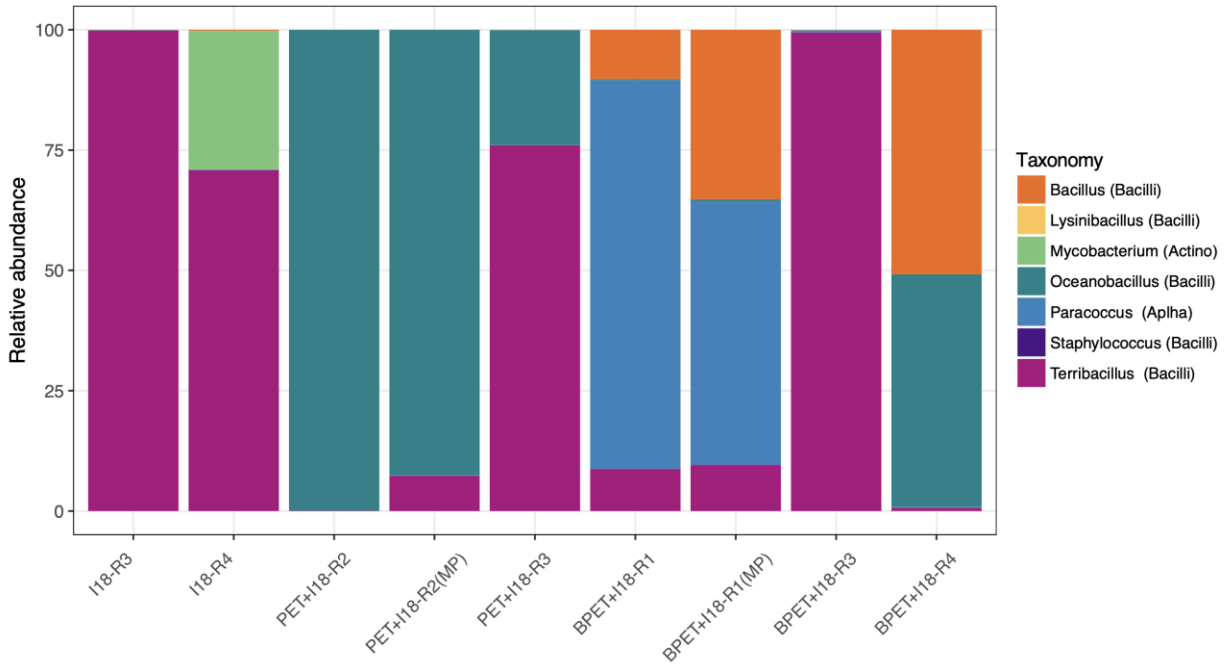

Figure 24. Relative abundance (%) of bacterial taxa at genus level (class within parenthesis) developed in the positive controls (I18) and microplastic samples inoculated with I18 after 90 days of incubation. MP refers to the bacteria found attached to the microplastic particles, as compared to free bacteria found in the surrounding marine broth (B).

3.4.2.2 *Identification of bacteria isolates*

For the purpose of associating isolates to accurately named species, a maximum likelihood phylogenetic tree based on the 16S rRNA gene was constructed by comparing the almost complete 16S rRNA gene sequences of the obtained bacterial isolates with the type strain (Palma et al., 2021). Based on the analysis of 16S rRNA by NCBI BLAST database, the isolates WC and YC was related to 16S rRNA genes of the members of the genus *Ureibacillus (Ureibacillus chungkukjangi*) with the sequence identity values of 99.5-100 % GenBank acession N^0s KP877500 (KP87750.1), KT 719580 (KT719580.1) and MK 389343 (MK389343.1) through a NCBI blast search (Table 8); according to the 16S rRNA gene sequence phylogeny, the isolates WC and YC, was assigned *Ureibacillus chungkukjangi* presents 98% similarity with its true strain revealing a closer relation (Figure. 25). Similarities among the two isolates suggest that both of them were phenotypically different but genetically similar (Jiménez, 1990; Waldemar, et al., 2005). The strain

identified also is similar to the previously isolated strains from deep sea sediments (Yu, et al., 2019). However, to our knowledge the identified strain have never been reported to degrade PET/BPET MPs.

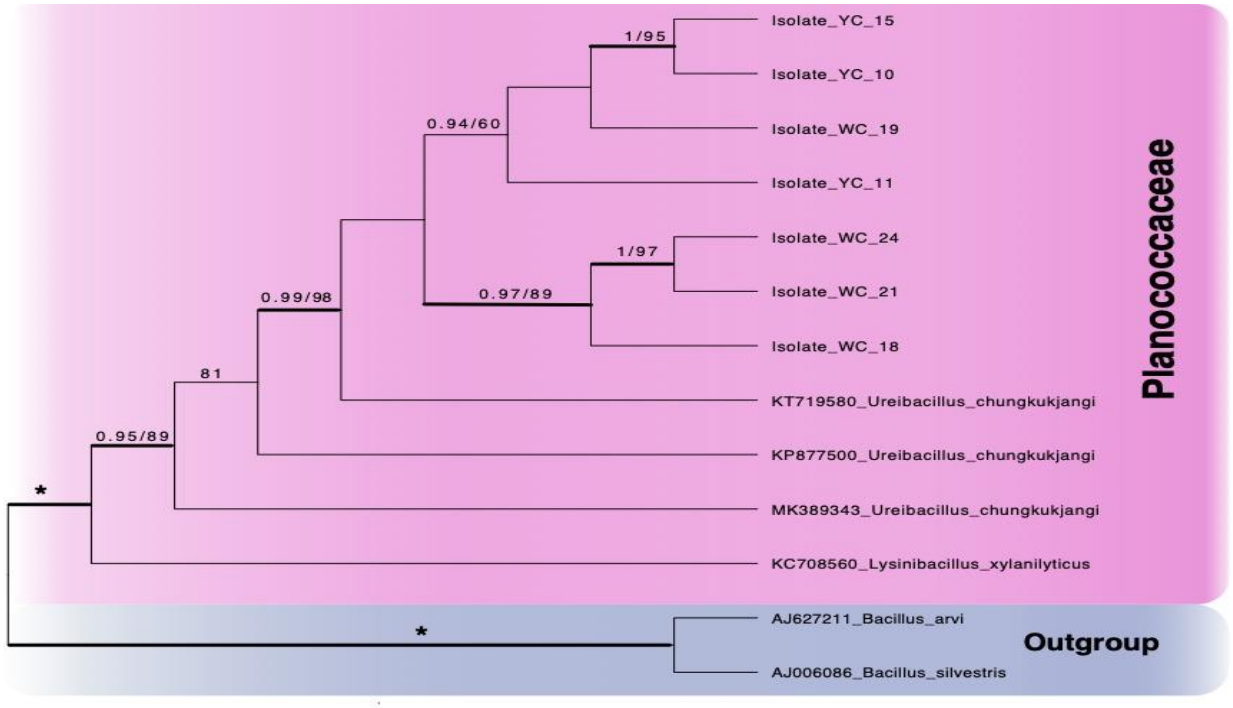

Figure 25. Phylogenetic tree based on based on Bayesian and Maximum likelihood analyses of 16S rRNA gene sequences. The two support values associated with each internal branch correspond to PPs and MLbs proportions, respectively. Branches in bold indicate a support of PP ≥ 0.95 and MLbs ≥ 70%. An asterisk on a bold branch indicates that this node has a support of PP = 1.0 and MLbs = 100. The tree was rooted using two species from *Viridibacillus*.

Table 8. Bacterial Identification using 16S rRNA gene sequence analysis of the bacteria isolates

SN	Isolate ID	Scientific name	Query cover (%)	Identity (%)	Accession N^{o}
1	YC	*Ureibacillus chungkukjangi*	100	99.5	KP877500.1
2	YC	*Ureibacillus chungkukjangi*		100	KT719580.1
3	YC	*Ureibacillus chungkukjangi*		100	KT719580.1
4	WC	*Ureibacillus chungkukjangi*		100	MK389343.1
5	WC	*Ureibacillus chungkukjangi*		100	KT719580.1
6	YC	*Ureibacillus chungkukjangi*		100	KT719580.1
7	WC	*Ureibacillus chungkukjangi*		100	KT719580.1

3.5. PET and BPET biodegradation/biofragmentation comparison

Overall, both MPs showed somewhat signs of biodegradation, or at least biodeterioration and biofragmentation after incubation with the bacterial consortium and isolates WC and YC, as shown by changes in the functional groups on the surface of the polymers (determined by FTIR-ATR), and the formation of cavities, scratches, fractures and biofilms on the surface of the MP films (determined by SEM). The COD showed, as it was hypothesized, that BPET was degraded very fast as it required more oxygen to be degraded in comparison to PET. Comparing the two samples, i.e., the PET/BPET MP samples treated with bacteria inoculum #I18, the rate of degradation as defined by spectral peaks, BPET samples treated with inoculum # I18 was statistically significantly higher than those of the PET. In addition to that, for both, PET/BPET MPs samples treated with bacteria inoculum #I18, the most significant statistical decrease and increase of the intensities of the spectral peaks were observed on day 28 of the experiment (Tables 2 and 5). This could have been influenced by higher optical densities and pH of both PET and BPET samples inoculated with bacteria community I18 on day 28.

4. CONCLUSIONS

This study has showed that the selected bacterial inoculum #I18 and isolates from that community have the potential to biodegrade, or at least biodeteriorate, petroleum-based and bio-based PET MPs in a similar way (at a very slow rate in both cases). Formation of new peaks, disappearance of peaks and or significant increase and decrease of peak intensities in the FTIR -ATR spectrum of the PET/BPET microplastics and consequent morphological changes observed in SEM images proved that the process of biodegradation and the ability of the bacteria inoculum #I18 and its isolates to grow on PET and BPET microplastics and utilize them as their carbon source. During the assay, an initial community of bacteria inoculum # I18 used in the experiment, which was mainly composed by the groups of *Arcobacter*, *Cutibacterium*, *Halodesulfovibrio*, *Marinobacter*, P*seudoalteromonas*, *Pseudomonas*, *Ruegeria*, *Shewanella*, *Tepidibacter* and *Vibrio*. However, after 90 days incubation, initial population suffered a shift with an increase in members assigned to the genus *Bacillus*, *Lysinibacillus*, *Mycobacterium*, *Oceanbacillus*, *Ornithinimicrobium*, *Paracoccus*, *Strepylococcus*, *Streptomyces* and *Teribacillus*, suggesting that the observed taxa were likely more resistant to BPET/PET MPs and could degrade or biofragment the PET/BPET MP and its metabolic products. These kinds of shifts or changes tends to occur when the bacteria communities, in our case #I18, are exposed to different substrates (in our case, PET/BPET MPs), since exposure to them lead to an adaptation and or modification/restructuring of the original consortium/community. One bacterial strain with the resistance and ability to grow in the presence of BPET/PET MP assigned to genus *Ureibacillus* (*Ureibacillus chungkukjangi*) was also identified from the isolates during the study.The strains identified in this study could be very useful in further biodegradation studies using PET and BPET microplastics as a sole carbon source. Furthermore, the findings of this study further highlight the importance of rethinking bioplastics as an alternative to conventional plastics and how biological recycling can provide a “green route” for PET microplastic pollution.

5. REFERENCES

Adyel, T. M. (2020). Accumulation of plastic waste during COVID-19. *SCIENCE*, 1314-1315.

Ahmaditabatabaei, S., Kyazze, G., Iqbal, H., & Keshavarz, T. (2021). Fungal Enzymes as Catalytic Tools for Polyethylene Terephthalate (PET) Degradation. *J.Fungi, 7*(931), 1-17.

Alfaro, M. E., Zoller, S., & Lutzoni, F. (2003). Bayes or Bootstrap? A Simulation Study Comparing the Performance of Bayesian Markov Chain Monte Carlo Sampling and Bootstrapping in Assessing Phylogenetic Confidence. *Molecular Biology and Evolution, 20*, 255-266.

Alshehrei, F. (2017). Biodegradation of Synthetic and Natural Plastic by Microorganisms. *Journal of Applied & Environmental Microbiology*, 8-19.

Ammala, A., Bateman, S., Dean, K., Petinakis, E., Sangwan, P., Wong, S., Leong, K. (2011). An overview of degradable and biodegradable polyolefins. *Progress in Polymer Science*, 1015-1049.

Andrady, A. L. (2017). The plastic in microplastics: A review. *Marine Pollution Bulletin*, 12-22.

Atkinson, J. R., Biddlestone, F., & Hay, J. N. (2000). An investigation of glass formation and physical ageing in poly(ethylene terephthalate) by FT-IR spectroscopy. *Polymer Communication*, 6965-6968.

Austin, H. P., Allen, M. D., Donohoe, B. S., Rorrer, N. A., Kearns, F. L., Silveira, R. L., Sk. (2018). Characterization and engineering of a plastic-degrading aromatic polyesterase. *PNAS*, 1-8.

Auta, H. S., Emenike, C. U., & Fauzia, S. H. (2017). Screening of Bacillus strains isolated from mangrove ecosystems in Peninsular Malaysia for microplastic degradation. *Environmental Pollution*, 1552-1559.

Auta, H. S., Emenike, C. U., Jayanthi, B., & Fauziah, S. H. (2018). Growth kinetics and biodeterioration of polypropylene microplastics by Bacillus sp. and Rhodococcus sp. isolated from mangrove sediment. *Marine Pollution Bulletin*, 15-21.

Auta, H., Obioye, O., Aransiola, S., Bala, J., Chukwuemeka, V., Hassan, A., Fauziah, S. (2022). Enhanced microbial degradation of PET and PS microplastics under natural conditions in mangrove environment. *Journal of Environmental Management*, 1-12.

Axelsson, C., & van Sebille, E. (2017). Prevention through policy: Urban macroplastic leakages to the marine environment during extreme rainfall events. *Marine Pollution Bulletin*, 211-227.

Bahl, S. K., Cornell, D. D., Boerio, F. J., & McGraw, G. E. (1974). Interpretation of the vibrational Spectra of Poly(Ethylene Terephthalate. *J. Polym. Sci.., 12*, 13-19.

Billig, S., Oeser, T., Birkemeyer, C., & Zimmermann, W. (2010). Hydrolysis of cyclic poly(ethylene terephthalate) trimers by a carboxylesterase from Thermobifida fusca KW3. *Appl Microbiol Biotechnol*, 1753-1764.

Benson, N. U., Bassey, D. E., & Palanisami, T. (2021). COVID pollution: impact of COVID-19 pandemic on global plastic waste footprint. *Heliyon, 7*(2), 1-9.

Bin, S., Patel, M., Yu, D., Yan, J., Li, Z., Petriw, D., Howe, J. Y. (2022). Automatic quantification and classification of microplastics in scanning electron micrographs via deep learning. *Science of The Total Environment*, 1-11.

Borchani, K. E., Carrot, C., & Jaziri, M. (2015). Biocomposites of Alfa fibers dispersed in the Mater-Bi® type bioplastic: Morphology, mechanical and thermal properties. *Composites Part A: Applied Science and Manufacturing*, 371-379.

Borrelle, S., Ringma, J., Law, K., Monnahan, C., Lebreton, L., McGivern, A., Roc. (2020). Predicted growth in plastic waste exceeds efforts to mitigate plastic pollution. *Science, 369*(6510), 1515-1518.

Boucher, J., Billard, G., Simeone, E., & Sousa, J. (2020). *The marine plastic footprint.* Retrieved from portals.iucn.org: https://portals.iucn.org/library/sites/library/files/documents/2020-001-En.pdf

Bretas Alvim, C., Bes-Piá, M. A., & Mendoza-Roca, J. A. (2020). Separation and identification of microplastics from primary and secondary effluents and activated sludge from wastewater treatment plants. *Chemical Engineering*, 1-10.

Brown, W. H., Foote, C. S., Iverson, B. L., & Anslyn, E. (2011). *Organic Chemistry.* Stamford, U.S.A: Cengage Learning.

Browne, M. A., Dissanayake, A., Galloway, T. S., Lowe, D. M., & Thompson, R. C. (2008). Ingested Microscopic Plastic Translocates to the Circulatory System of the Mussel, Mytilus edulis (L.). *Environ. Sci. Technol.*, 5026-5031.

Carniel, A., Valoni, É., Nicomedes Junior, J., Gomes, A. d., & de Castro, A. d. (2017). Lipase from Candida antarctica (CALB) and cutinase from Humicola insolens act synergistically for PET hydrolysis to terephthalic acid. *Process Biochemistry*, 84-90.

Carr, C. M., Clarke, D. J., & Dobson, A. D. (2020). Microbial Polyethylene Terephthalate Hydrolases: Current and Future Perspectives. *Front. Microbiol.*, 1-23.

Carson, H. S., Nerheim, M. S., Carroll, K. A., & Eriksen, M. (2013). The plastic-associated microorganisms of the North Pacific Gyre. *Marine Pollution Bulletin* , 126-132.

Chen, Q., Allgeier, A., Yin, D., & Hollert, H. (2019). Leaching of endocrine disrupting chemicals from marine microplastics and mesoplastics under common life stress conditions. *Environment International*, 1-9.

Chen, T., Zhang, W., & Zhang, J. (2015). Alkali resistance of poly(ethylene terephthalate) (PET) and poly(ethylene glycol-co-1,4-cyclohexanedimethanol terephthalate) (PETG) copolyesters: The role of composition. *Polymer Degradation and Stability*, 232-243.

Chen, Z., Wang , Y., Cheng, Y., Wang, X., & Tong , S. (2020). Efficient biodegradation of highly crystallized polyethylene terephthalate through cell surface display of bacterial PETase. *Science of the Total Environment*, 1-9.

Cole, K. C., Ajji, A., & Pellerin, E. (2002). New Insights into the Development of Ordered Structure in Poly(ethylene terephthalate). 1. Results from External Reflection Infrared Spectroscopy. *Macromolecules* , 770-784.

Cole, K. C., Guèvremont, J., Ajji, A., & Dumoulin, M. M. (1994). Characterization of Surface Orientation in Poly(ethylene terephthalate) by Front-Surface Reflection Infrared Spectroscopy. *Appl.Spectrosc*, 1513-1521.

Cole, M., Lindeque, P., Fileman, E., Halsband, C., Goodhead, R., Moger, J., & Galloway, T. S. (2013). Microplastic Ingestion by Zooplankton. *Environ. Sci. Technol.*, 6646−6655.

Comeau, A., Douglas, G., & Langille, M. (2017). Microbiome helper: a custom and streamlined workflow for microbiome research. *mSystems 2*, 00127-16.

Cox, K. D., Covernton, G. A., Davies, H. L., Dower, J. F., Juanes, F., & Dudas, S. E. (2019). Human Consumption of Microplastics. *Emviron. Sci. Technol.*, 7068-7074.

Dai , L., Qu, Y., Huang, J.-W., Hu, Y., Hu, H., Li, S., & Chen, C.-C. (2021). Enhancing PET hydrolytic enzyme activity by fusion of the cellulose–binding domain of cellobiohydrolase I from Trichoderma reesei. *Journal of Biotechnology*, 1-4.

Dang, T. C., Nguyen, D. T., Thai, H., Nguyen, T. C., Tran, T. T., Le, V. H., Nguyen, Q. T. (2018). Plastic degradation by thermophilic Bacillus sp. BCBT21 isolated from composting agricultural residual in Vietnam. *Adv. Nat. Sci.: Nanosci. Nanotechnol*, 1-11.

Denaro, R., Aulenta, F., Crisafi, F., Di Pippo, F., Cruz Viggi, C., Matturro, B.,Rossetti, S. (2020). Marine hydrocarbon-degrading bacteria breakdown poly(ethylene terephthalate) (PET). *Science of the Total Environment*, 1-16.

Dhote , M., Juwarkar, A., Kumar, A., Kanade, G. S., & Chakrabarti, T. (2010). Biodegradation of chrysene by the bacterial strains isolated from oily sludge. *World J Microbiol Biotechnol*, 329-355.

Dimassi, S. N., Hahladakis, J. N., Yahia , M. N., Ahmad , M. I., Sayadi, S., & Al-Ghouti, M. A. (2022). Degradation-fragmentation of marine plastic waste and their environmental implications: A critical review. *Arabian Journal of Chemistry*, 1-31.

Djebara, M., Stoquert, J. P., Abdesselam, M., Muller, D., & Chami, A. C. (2012). FTIR analysis of polyethylene terephthalate irradiated by MeV He+. *Nuclear Instruments and Methods in Physics Research B*, 70-77.

Donelli, I., Freddi, G., Nierstrasz, V. A., & Taddei, P. (2010). Surface structure and properties of poly-(ethylene terephthalate) hydrolyzed by alkali and cutinase. *Polymer Degradation and Stability*, 1542-1550.

Euginio, E. d., Campisano, I. S., de Castro, A. M., Coelho, M. A., & Langone, M. A. (2021). Experimental and mathematical modeling approaches for biocatalytic post-consumer poly(ethylene terephthalate) hydrolysis. *Journal of Biotechnology*, 1-10.

Europeanbioplastic. (2018, July). *What are bioplastic.* Retrieved May 2022, from European-bioplastic.org: https://docs.european-bioplastics.org/publications/fs/EuBP_FS_What_are_bioplastics.pdf

Fadare, O. O., & Okoffo, E. D. (2020). Covid-19 face masks: A potential source of microplastic fibers in the environment. *Science of the Total Environment*, 1-4.

Farzi, A., Dehnad, A., & Fotouhi, A. F. (2019). Biodegradation of polyethylene terephthalate waste using Streptomyces species and kinetic modeling of the process. *Biocatalysis and Agricultural Biotechnology*, 25-31.

Fernández de Villalobos, N., Costa, M. C., & Marín-Beltrán, I. (2022). A community of marine bacteria with potential to biodegrade petroleum-based and biobased microplastics. *Marine Pollution Bulletin, 185, Part A,*, 1-15.

Fotopoulou, K., & Karapanagioti, H. K. (2017). Degradation of various plastics in the environment. *Hazardous chemicals associated with plastics in the marine environment*, 71-92.

Gao, R., & Sun, C. (2021). A marine bacterial community capable of degrading poly(ethylene terephthalate) and polyethylene . *Journal of Hazardous Materials*, 1-12.

Geyer, R., Jambeck, J. R., & Law, K. L. (2017). Production, use, and fate of all plastics ever made. *Sci.Ad*, 1-5.

Gong, J., Kong, T., Li, Y., Li, Q., Li, Z., & Zhang, J. (2018). Biodegradation of Microplastic Derived from Poly(ethylene terephthalate) with Bacterial Whole-Cell Biocatalysts. *polymers*, 1-13.

Gouin, T., Roche, N., Lohmann, R., & Hodges, G. (2011). A Thermodynamic Approach for Assessing the Environmental Exposure of Chemicals Absorbed to Microplastic. *Environ. Sci. Technol.*, 1466-1472.

Gourmelon, G. (2015, 01 27). *Global Plastic Production Rises, Recycling Lags.* Retrieved from vitalsigns.worldwatch.org: http://www.plastic-resource-center.com/wp-content/uploads/2018/11/Global-Plastic-Production-RisesRecycling-Lags.pdf

Gregory, M. R. (2009). Review:Environmental implications of plastic debris in marine settings—entanglement, ingestion, smothering, hangers-on, hitch-hiking and alien invasions. *Phil. Trans. R. Soc. B*, 2013-2025.

Hahladakis, J. N., Velis, C. A., Weber, R., Iacovidou, E., & Purnell, P. (2018). An overview of chemical additives present in plastics: Migration, release, fate and environmental impact during their use, disposal and recycling. *Journal of Hazardous Materials*, 179-199.

Harshvardhan, K., & Jha, B. (2013). Biodegradation of low-density polyethylene by marine bacteria from pelagic waters, Arabian Sea, India. *Marine Pollution Bulletin*, 100-106.

Hatzonikolakis, Y., Giakoumi, S., Raitsos, D., Tsiaras, K., Kalaroni, S., Triantaphyllidis, G., & Triantafyllou, G. (2022). Quantifying Transboundary Plastic Pollution in Marine Protected Areas Across the Mediterranean Sea. *Front. Mar. Sci.*, 1-17.

Hillis, D. M., & Bull, J. J. (1993). An empirical test of bootstrapping as a method for assessing confidence in phylogenetic analysis. *Syst. Biol.*, 182-192.

Hirota, Y., Hayashi, K., Kawanishi, T., & Takiguchi, N. (2020). Effect of pH on Hydrolysis of Biodegradable Polyethylene Terephthalate. *Journal of Chemical Engineering of Japan, 56*(6), 267-272.

Hoffmann, J., Reznihikovi, I., Vanokova, S., & Kupec, J. (1997). Manometric Determination of Biological Degradability of Substances Poorly Soluble in Aqueous Environments. *International Bhdeterioration & Biodegradation*, 327-332.

Holland, B. J., & Hay, J. N. (2002). The thermal degradation of PET and analogous polyesters measured by thermal analysis±Fourier transform infrared spectroscopy. *Polymer, 43*, 1835-1847.

House–Ambrosetti, T. E. (2014). he Excellence of the Plastics Supply Chain in Relaunching Manufacturing in Italy and Europe. Milan, Italy.

Ioakeimidis, C., Fotopoulou, K. N., Karapanagioti, H. K., Geraga, M., Zeri, C., Papathanassiou, E., Papatheodorou, G. (2016). The degradation potential of PET bottles in the marine environment: An ATR-FTIR based approach. *Sci. Rep., 6*, 1-8.

Janczak, K., Dabrowska, G. B., Raszkowska-Kaczor, A., Kaczor, D., Hrnkiewicz, K., & Richert, A. (2020). Biodegradation of the plastics PLA and PET in cultivated soil with the participation of microorganisms and plants. *International Biodeterioration & Biodegradation*, 1-10.

Jeon, J.-M., Choi, T.-R., Park, J.-H., Yang, Y.-H., & Yoon, J.-J. (2021). Biodegradation of polyethylene and polypropylene by Lysinibacillus species JJY0216 isolated from soil grove. *Polymer Degradation and Stability, 191*, 1-8.

Jia, Y., Samak, N. A., Hao, X., Chen, Z., Gama, Y., Zhao, X., Xing, J. (2021). Nano-immobilization of PETase enzyme for enhanced polyethylene terephthalate biodegradation. *Biochemical Engineering Journal*, 1-8.

Jiménez , L. (1990). Molecular analysis of deep-subsurface bacteria. *Appl Environ Microbiol*, 2108-13.

Jones Jr., M., & Fleming, S. A. (2014). *Organic Chemistry, 5th ed.* W. W. Nor- ton & Company: New York, U.S.A.

Joo, S., Cho, I. J., Seo, H., Son, H. F., Sagong, H.-Y., Shin, T. J., Kim, K.-J. (2018). Structural insight into molecular mechanism of poly (ethylene terephthalate) degradation. *NATURE COMMUNICATION, 9*(382), 1-12.

Jung, M. Y., Kim, J.-S., Paek, W. K., Styrak, I., Park, I., Sin, Y., Chang, Y. (2012). Description of Lysinibacillus sinduriensis sp. nov., and transfer of Bacillus massiliensis and Bacillus odysseyi to the genus *Lysinibacillus* as *Lysinibacillus massiliensis comb*. nov. and *Lysinibacillus odysseyi* comb. nov. with emended description of the g. *International Journal of Systematic and Evolutionary Microbiology* , 2347-2355.

Jung, M. R., Horgen, F. D., Orsk, S. V., Rodriguez, V. C., Beers, K. L., Balazs, G. H.,Lynch. (2018). Validation of ATR FT-IR to identify polymers of plastic marine debris, including those ingested by marine organisms. *Marine Pollution Bulletin*, 704-716.

Krzan, A., Hemjinda, S., Miertus, S., Corti, A., & Chiellini, E. (2006). Standardization and certification in the area of environmentally degradable plastics. *Polymer Degradation and Stability*, 2819-2833.

Kubowicz, S., & Booth, A. M. (2017). Biodegradability of Plastics: Challenges and Misconceptions. *Environ. Sci. Technol., 51*, 12058-12060.

Kumar, A. G., Hinduja, M., Sujitha, K., Rajan, N. N., & Dharani, G. (2021). Biodegradation of polystyrene by deep-sea Bacillus paralicheniformis G1 and genome analysis. *Science of the Total Environment* , 1-9.

Kumar, R., Verma, A., Shome, A., Sinha, R., Sinha, S., Jha, P. K.,Prasad, V. P. (2021). Impacts of Plastic Pollution on Ecosystem Services, Sustainable Development Goals, and Need to Focus on Circular Economy and Policy Interventions. *Sustainability*, 1-40.

Kvale, K., Prowe, A. E., Chien, C. -T., Landolfi, A., & Oschlies, A. (2021). Zooplankton grazing of microplastic can accelerate global loss of ocean oxygen. *Nature Communications*, 1-8.

Larsson, K. (2007). Re-thinking the classification of corticioid fungi. *Mycol Res. III, 9*, 1040-1063.

Lebaron, P., Ghiglione, J.-F., Fajon, C., Batailler, N., & Normand, P. (1998, March). Phenotypic and genetic diversity within a colony morphotype,. *FEMS Microbiology Letters, 160*(1), 137-143.

Li, L., Zhao, X., Li, Z., & Song, K. (2021). COVID-19: Performance study of microplastic inhalation risk posed by wearing masks. *Journal of Hazardous Materials*, 1-9.

Li, Z., Chen, K., Yu, L., Shi, Q., & Sun, Y. (2022). Fe3O4 nanoparticles-mediated solar-driven enzymatic PET degradation with PET hydrolase. *Biochemical Engineering Journal*, 1-9.

Liu, P., Zhang, T., Zheng, Y., Li, Q., Su, T., & Q, Q. (2021). Potential one-step strategy for PET degradation and PHB biosynthesis through co-cultivation of two engineered microorganisms. *Engineering Microbiology*, 1-8.

Lucas , N., Bienaime, C., Belloy, C., Queneudec, M., Silvestre , F., & Nava-Saucedo, J.-E. (2008). Polymer biodegradation: Mechanisms and estimation techniques. *Chemosphere*, 429-442.

Martinez, J., Smith, D. C., Steward, C. F., & Azam, F. (1996). Variability in ectohydrolytic enzyme activities of pelagic marine bacteria and its significance for substrate processing in the sea. *Aquat Microb Ecol*, 223-230.

Marín-Beltrán, I., Demaria , F., Ofelio, C., Serra, L. M., Turiel, A., Ripple, W. J., Costa, M. (2022). Scientists' warning against the society of waste. *Science of the Total Environment*, 1-14.

Maurya, A., Bhattacharya, A., & Khare, S. (2020). Enzymatic Remediation of Polyethylene Terephthalate (PET)–Based Polymers for Effective Management of Plastic Wastes: An Overview. *Front. Bioeng. Biotechnol.*, 1-13.

Mecozzi, M., & Nisini, L. (2019). The differentiation of biodegradable and non-biodegradable polyethylene terephthalate (PET) samples by FTIR spectroscopy: A potential support for the structural differentiation of PET in environmental analysis. *Infrared Physics & Technology*, 119-126.

Miyake, A. (1959). The Infrared Spectrum of Polyethylene Terephthalate. II. Polyethylene-d4 Terephthalate. *J. Polym. Sci.*, 497-512.

Mohanan, N., Montaze, Z., Sharma, P. K., & Levin, D. B. (2020). Microbial and Enzymatic Degradation of Synthetic Plastics. *Front. Microbiol*, 1-22.

Moreira, I., Ribeiro, A., Afonso, C., Tiritan, M., & Castro , P. (2014). Enantio-selective biodegradation of fluoxetine by the bacterial strain Labrys portucalensis F11. *Chemosphere*, 103-111.

Moshood, T. D., Nawanir, G., Mahmud, F., Mohamad, F., Ahmad, M. H., & AbdulGhani, A. (2022). Sustainability of biodegradable plastics: New problem or solution to solve the global plastic pollution? *Current Research in Green and Sustainable Chemistry*, 1-18.

Nechwatal, A., Blokesch, A., Nicolai, M., Krieg, M., Kolbe, A., Wolf, M., & Gerhardt, M. (2006). A Contribution to the Investigation of Enzyme-Catalysed Hydrolysis of Poly(ethylene terephthalate) Oligomers. *Macromol. Mater. Eng*, 1486-1494.

Nimchua, T., Punnapayak, H., & Zimmermann, W. (2007). Comparison of the hydrolysis of polyethylene terephthalate fibers by a hydrolase from Fusarium oxysporum LCH I and Fusarium solani f. sp. pisi. *Biotechnol. J.*, 361–364.

NOAA. (2021, February 26). *How much oxygen comes from the ocean?* Retrieved from oceanservice.noaa.gov: https://oceanservice.noaa.gov/facts/ocean-oxygen.html

Nylander, J. A. (2004). MrModeltest v2. Program distributed by the author. *Evolutionary Biology Centre, Uppsala University.*, 1-2.

Oberbeckmann, S., Loeder, M. G., Gerdts, G., & Osborn, A. M. (2014). Spatial and seasonal variation in diversity and structure of microbial biofilms on marine plastics in Northern European waters. *FEMS Microbiol Ecol, 90*, 478-492.

OECD. (2022). Global Plastics Outlook: Economic Drivers, Environmental Impacts and Policy Options. *OECD Publishing*, 1-201.

Ojha, N., Pradhan, N., Singh, S., Barla, A., Shrivastava, A., Khatua, P., Bose, S. (2017). Evaluation of HDPE and LDPE degradation by fungus, implemented by statistical optimization. *Sci Rep*, 1-13.

Olatayo, K. I., Mativenga, P. T., & Marnewick, A. L. (2021). COVID-19 PPE plastic material flows and waste management: Quantification and implications for South Africa. *Science of the Total Environment, 790*, 1-13.

Oliveira, J., Belchior , A., da Silva, V. D., Rotter, A., Zeljko, P., Almeida, P. L., Gaudencio, S. P. (2020). Marine Environmental Plastic Pollution: Mitigation by Microorganism Degradation and Recycling Valorization. *Front.Mar. Sci*, 1-35.

Pagga, U. (1997). Testing biodegradability with standardized methods. *Chemosphere*, 2953-2972.

Paliy, O., Kenche, H., Abernathy, F., & Michail, S. (2009). High-throughput quantitative analysis of the human intestinal microbiota with a phylogenetic microarray. *Appl. Environ. Microbiol*, 3572-3579.

Palma, T., Shylova, A., Carlier, J. D., & Costa, M. (2021). An autochthonous aerobic bacterial community and its cultivable isolates capable of degrading fluoxetine. *J Chem Technol Biotechnol* , 2813-2826.

Parashar, N., & Hait, S. (2011). Plastics in the time of COVID-19 pandemic: Protector or polluter? *Science of The Environment, 759*, 1-15.

Patrício Silva, A. L., Prata, J. C., Duarte, A. C., Barcelo, D., & Rocha-Santos, t. (2021). An urgent call to think globally and act locally on landfill disposable plastics under and after covid-19 pandemic: Pollution prevention and technological (Bio) remediation solutions. *Chemical Engineering Journal, 426*(131201), 1-12.

Peng, Y., Wu, P., Schartup, A. T., & Zhang, Y. (2021). Plastic waste release caused by COVID-19 and its fate in the global ocean. *PNAS*, 1-6.

Pinto da Costa, J. (2021). The 2019 global pandemic and plastic pollution prevention measures: Playing catch-up. *Science of The Total Environment*, 1-5.

Plasticseurope. (2021, Dec 20). *Plastics-the Facts 2021*. Retrieved from plasticseurope.org: https://plasticseurope.org/knowledge-hub/plastics-the-facts-2021/

Raushan, K., Pratik, M., & Eswara, P. (2022, July). *Bioplastic Market by Type (Biodegradable Plastic and Non-biodegradable Plastic) and Application (Flexible Packaging, Rigid Packaging, Textiles, Coatings & Adhesives, Agriculture & Horticulture, Consumer Goods, and Others):*. (Allied Market Research) Retrieved February 24, 2022, from www.alliedmarketresearch.com: https://www.alliedmarketresearch.com/bioplastics-market

Reese, G. (2003). *Modern Polyesters: Chemistry and Technology of Polyesters and Copolyesters*. (J. Scheirs, & T. E. Long, Eds.) West Sussex: John Wiley & Sons Ltd.

Ribitsch, D., Heumann, S., Trotscha, E., Acero, E. H., Gramiel, K., Leber, R., Freddi. (2011). Hydrolysis of Polyethyleneterephthalate by p-Nitrobenzylesterase from Bacillus subtilis. *Biotechnology Progress, 00*, 1-9.

Roberts, C., Edwards, S., Vague, M., León-Zayas, R., Scheffer, H., Chan, G., Mellie, J. (2020). Environmental Consortium Containing Pseudomonas and Bacillus Species Synergistically Degrades Polyethylene Terephthalate Plastic. *mSphere*.

Rochman, C. M., Cook, A.-M., & Koelmans, A. A. (2016). Plastic Debris and Policy: Using Current Scientific Understanding to Invoke Positive Change. *Environmental Toxicology and Chemistry*, 1617-1626.

Ronquist, F., & Huelsenbeck, J. P. (2003). MrBayes 3: Bayesian phylogenetic inference under mixed models. *Bioinformatics, 19*, 1572-1574.

Saimmai, A., Tani, A., Sobhon, V., & Maneerat, S. (2012). Mangrove sediment, a new source of potential biosurfactant-producing bacteria. *Ann Microbiol, 62*, 1669-1679.

Sammon, C., Yarwood, J., & Everall, N. (2000). A FTIR–ATR study of liquid diffusion processes in PET films: comparison of water with simple alcohols. *Polymer* , 2531-2534.

Sanniyasi, E., Gopal, R. K., Gunasekar, D. K., & Raj, P. P. (2021). Biodegradation of low-density polyethylene (LDPE) sheet by microalga, Uronema africanum Borge. *Scientific Reports*, 1-33.

Sarkhel, R., Sengupta, S., Das, P., & Bhowal, A. (2020). Comparative biodegradation study of polymer from plastic bottle waste using novel isolated bacteria and fungi from marine source. *Journal of Polymer Research*, 1-8.

Shah, A. A., Hasan, F., Hameed, A., & Ahmed, S. (2008). Biological degradation of plastics: A comprehensive review. *Biotechnology Advances*, 246-265.

Shamz, M., Alam, I., & Mahbub, M. (2011). Plastic pollution during COVID-19: Plastic waste directives and its long-term impact on the environment. *Environmental Advances*, *5*(100119), 1-11.

Sharon, C., & Sharon, M. (2012). Studies on Biodegradation of Polyethylene terephthalate: A synthetic polymer. *J. Microbiol. Biotech. Res*, 248-257.

Shen, M., Ye, S., Zeng, G., Zhang, Y., Xing, L., Tang, W., . . . Liu, S. (2019). Can microplastics pose a threat to ocean carbon sequestration? *Marine Pollution Bulletin*, 1-3.

Sheng , C., Tong, X., Woodard, R. W., Du, G., & Chen, J. (2008). Identification and Characterization of Bacterial Cutinase. *Journal of biological Chemistry*, 25854-25862.

Sivan, A., Szanto, M., & Pavlov, V. (2006). Biofilm development of the polyethylene-degrading bacterium Rhodococcus ruber. *Appl Microbiol Biotechnol*, 346–352.

Skariyachan, S., Patil, A. A., Shankar, A., Manjunath, M., Bachappanavar, N., & Kiran, S. (2018). Enhanced polymer degradation of polyethylene and polypropylene by novel thermophilic consortia of Brevibacillus sps. and Aneurinibacillus sp. screened from waste

management landfills and sewage treatment plants. *Polymer Degradation and Stability*, 52-68.

Socrates, G. (1994). *Infrared characteristic group frequencies table and chart. 2nd ed.* Baffins Lane, Chichester, England: John Wiley & Sons.

Son, H. F., Seo, H., Hong, H., Lee, D., & Kim, K.-J. (2021). Implications for the PET decomposition mechanism through similarity and dissimilarity between PETases from Rhizobacter gummiphilus and Ideonella sakaiensis. *Journal of hazardous Materials*, 1-7.

Sriromreun, P., Petchsuk, A., Opaprakasit, M., & Opaprakasit, P. (2013). Standard methods for characterizations of structure and hydrolytic degradation of aliphatic/aromatic copolyesters,. *Polymer Degradation and Stability, 98*(1), 169-176.

Stamatakis, A. (2014). RAxML version 8: a tool for phylogenetic analysis and post-analysis of large phylogenies. *Bioinformatics, 30*(9), 1312-1313.

Steven, S., Octiano, I., & Mardiyati, Y. (2020). Cladophora algae cellulose and starch based bio-composite as an alternative for environmentally friendly packaging material. *AIP Conference Proceedings* (p. 40006). AIP Publishing LLC.

Sulaiman, S., Yamamoto, S., Kanaya, E., Kim, J.-J., Koga, Y., Takano, K., & Kanaya, S. (2011). Isolation of a Novel Cutinase Homolog with Polyethylene Terephthalate-Degrading Activity from Leaf-Branch Compost by Using a Metagenomic Approach. *Applied and Environmental Microbiology*, 1556-1562.

Taniguchi, I., Yoshida, S., Hiraga, K., Miyamoto, K., Kimura, Y., & Oda, K. (2019). Biodegradation of PET: Current Status and Application Aspects. *ACS Catal.*, 4089-4105.

TheGlobalist. (2015, December 9). *The Rise of Plastic The past, present and future of plastic production.* Retrieved from www.theglobalist.com: https://www.theglobalist.com/the-rise-of-plastic/

Thompson, R. C., Olsen, Y., Mitchel, R. P., Davis, A., Rowland, S. J., John, A. W., Russell, A. E. (2004). Lost at sea: where is all the plastic? *Science*, 838.

Tiseo , I. (2022, July 27). *Global plastic market size value 2021-2030.* Retrieved from Statista.com: https://www.statista.com/statistics/1060583/global-market-value-of-plastic/

Tiwari, A. K., Gautam , M., & Maurya, H. K. (2018). Recent development of biodegradation techniques of polymer. *International Journal of Research - Granthaalayah, 6*(6), 414-452.

Torena, P., Alvarez-Cuenca, M., & Reza, M. (2021). Biodegradation of polyethylene terephthalate microplastics by bacterial communities from activated sludge. *Can J Chem Eng*, 1-14.

UNESCO. (2022, May 09). *Ocean plastic pollution an overview: data and statistics.* Retrieved from Ocean Literacy Portal: https://oceanliteracy.unesco.org/plastic-pollution-ocean/

Van Cauwenberghe, L., & Janssen, C. R. (2014). Microplastics in bivalves cultured for human consumption. *Environ. Pollut.*, 65-70.

Venkatachalam, S., Nayak, S. G., Labde, J. V., Gharal, P. R., Rao , K., & Kelkar, A. K. (2012). Degradation and Recyclability of Poly (Ethylene Terephthalate). In H. E.-D. Saleh, *Polyester.* IntechOpen.

Waldemar, A., Heckel, F., Saha-Mo¨ller, C. R., Taupp, M., Meyer, J.-M., & Schreier, P. (2005). Opposite Enantioselectivities of Two Phenotypically and Genotypically Similar Strains of Pseudomonas frederiksbergensis in Bacterial Whole-Cell Sulfoxidation. *Appl Environ Microbiol*, 2199-2202.

Ward, I. M., & Wilding, M. A. (1977). Infra-red and Raman spectra of poly(m-methylene terephthalate) polymers. *Polymer, 18*, 327-335.

WEF. (2022, January 19). *We know plastic pollution is bad – but how exactly is it linked to climate change?* Retrieved from www.weforum.org: https://www.weforum.org/agenda/2022/01/plastic-pollution-climate-change-solution/

Woodall, L. C., Sanchez-Vidal, A., Canals, M., Paterson, G. L., Coppock, R., Sleight, V., Woodall, L. C. (2014). The deep sea is a major sink for microplastic debris. *R. Soc. open sci.*, 1-8.

Xu, L., Crawford, K., & Gorman, C. B. (2011). Effects of Temperature and pH on the Degradation of Poly(lactic acid) Brushes. *Macromolecules*, 4777-4782.

Yakimov , M. M., Timmis , K. N., & Golyshin , P. N. (2007). Obligate oil-degrading marine bacteria. *Curr. Opin. Biotech., 18*, 257-266.

Yu, L., Tang, X., Wei, S., Qiu, Y., Xu, X., Xu, G., Yang, Q. (2019). Isolation and characterization of a novel piezotolerant bacterium Lysinibacillus yapensis sp. nov., from deep-sea sediment of the Yap Trench, Pacific Ocean. *Journal of Microbiology*, 562-568.

Yuan, Z., Nag, R., & Cummins, E. (2022). Human health concerns regarding microplastics in the aquatic environment - From marine to food systems. *Science of the Total Environment*, 1-19.

Zannat, M. (2021). *Enhanced hydrolysis of polyethylene terephthalate (PET) plastics by ozone and ultrasound pretreatment.* Retrieved from https://knowledgecommons.lakeheadu.ca/handle/2453/4811

Zhang, M., Zhao, Y., Qin, X., Jia, W., Chai, L., Huang, M., & Huang, Y. (2019). Microplastics from mulching film is a distinct habitat for bacteria in farmland soil. *Science of the Total Environment*, 470-478.

Zheng, Y., Yanful , E. K., & Amarjeet , B. S. (2005). A Review of Plastic Waste Biodegradation. *Critical Reviews in Biotechnology*, 243-250.

Zhou, D., Chen, J., Wu, J., Yang, J., & Wang, H. (2021). Biodegradation and catalytic-chemical degradation strategies to mitigate microplastic pollution. *Sustainable materials and Technologies*, 1-14.

ANNEX:

A.Concentration of DNA of the bacterial isolates adhered to the MPs particles after 45days of incubation, as determined by Nanodrop spectrophotometry. YC and WC stands for the isolates with Yellow and White colonies and R corresponds to each replicate.

SAMPLE MPS	[DNA] (NG/μL)	A_{260}/A_{280}	A_{260}/A_{230}
YC-R1	2	2.36	0.09
YC-R2	3.4	1.93	0.28
YC -R3	1.6	4.91	0.16
WC-R1	2.1	1.66	0.13
WC-R2	1.2	3.05	0.02
WC-R3	2.1	1.70	0.07
PET+YC-R1	2.5	1.38	0.17
PET+YC-R2	2.1	1.05	0.12
PET+YC-R3	2.1	1.23	0.04
PET+ WC -R1	0.5	27.06	0.02
PET+ WC -R2	0.9	1.07	0.05
PET+ WC -R3	1.9	0.84	0.09
BPET+ YC -R1	0.4	45.90	0.05
BPET+YC -R2	1.9	1.22	0.09
BPET+ WC -R1	0.6	5.32	0.02
BPET+WC-R2	2.7	1.36	0.10